SOLID-LIQUID MASS TRANSFER FROM SPINNING SPHERE IN NON-NEWTONIAN LIQUID

BY

Abdullah M. Baduraig

A Thesis Presented to the
DEANSHIP OF GRADUATE STUDIES

KING FAHD UNIVERSITY OF PETROLEUM & MINERALS

DHAHRAN, SAUDI ARABIA

In Partial Fulfillment of the
Requirements for the Degree of

MASTER OF SCIENCE

In

CHEMICAL ENGINEERING DEPARTMENT

May 2013

KING FAHD UNIVERSITY OF PETROLEUM & MINERALS

DHAHRAN- 31261, SAUDI ARABIA

DEANSHIP OF GRADUATE STUDIES

This thesis, written by **Abdullah Mohsin Baduraig** under the direction his thesis advisor and approved by his thesis committee, has been presented and accepted by the Dean of Graduate Studies, in partial fulfillment of the requirements for the degree of **MASTER OF SCIENCE IN CHEMICAL ENGINEERING.**

Dr. S. U. Rahman
(Advisor)

Dr. Usamah A. Al-Mubaiyedh
Department Chairman

Dr. Usamah A. Al-Mubaiyedh
(Member)

Dr. Salam A. Zummo
Dean of Graduate Studies

Dr. Ibnelwaleed Ali Hussein
(Member)

26/5/13
Date

Dedicated to

My lovely family, my wife and my Parents in law

ACKNOWLEDGMENTS

Acknowledgement is due to King Fahd University of Petroleum & Minerals for providing me with this opportunity of research to continue my graduate degree. I am indebted to the department of Chemical Engineering in KFUPM. The facilities and support of the department made my work easier.

I am thankful to my thesis advisor professor S. U. Rahman. He was always there to assist and support. I have learned so much working with him. I am also thankful to committee members from KFUPM, Professor Ibnelwaleed Ali Hussein and Dr. Usamah A. Al-Mubaiyedh.

I am also thankful to Dr. Ahmad Al-Amer, Dr. Safdar Hosain, Mr. Adel Al-Amoudi, Mr. Abdulsamad Iddrisu and Mr. Mariano Gica, for their cooperation.

Special thanks to my parents for their prayers and support during this work. My brother, sisters and my wife were always there for me and have encouraged me during my entire course of study at KFUPM.

My friends at KFUPM Hasan Asiri, Osamah Bin-Dahman , Khalid Elkarsani, Faisal Al-Khelafi and the graduate students in the Chemical Engineering Department were always supportive.

TABLE OF CONTENTS

ACKNOWLEDGMENTS ..... **V**

TABLE OF CONTENTS ..... **VI**

LIST OF TABLES ..... **VIII**

LIST OF FIGURES ..... **IX**

LIST OF ABBREVIATIONS ..... **XI**

ABSTRACT ..... **XIII**

CHAPTER 1 INTRODUCTION **1**

1.1 Motivation **2**

1.2 Research Objective **3**

CHAPTER 2 LITERATURE REVIEW **4**

2.1 Limiting Diffusion Current Technique (LDCT) **4**

2.2 Mass Transfer Coefficient from Sphere **7**

2.2.1 Newtonian Fluid **7**

2.2.2 Non-Newtonian Fluid **9**

2.3 Mass Transfer Coefficient from spinning sphere **13**

2.3.1 Newtonian Fluid **14**

2.4 Electrochemical Method **17**

2.4.1 Cyclic Voltammetry **17**

2.4.2 Choronoamperometry **17**

CHAPTER 3 EXPERIMENTAL SET-UP AND METHODOLOGY **19**

3.1 The Experimental Set-Up **19**

3.2 Methodology of Performing the Experiment 25

4 CHAPTER 4 PHYSICAL PROPERTIES 27

4.1 Viscosity Measurement 27

4.2 Diffusion Coefficient Measurement 34

CHAPTER 5 RESULTS AND DISSCUSION 38

5.1 Polarization Curves 39

5.2 Chronoamperometric Curves 41

5.3 Newtonian Fluid 41

5.4 Non-Newtonian Fluid 48

5.4.1 Polarization Curve 48

5.4.2 Effect of Spheres Diameter 48

5.4.3 Effect of Rotational Speed 51

5.4.4 Effect of Adding CMC to the Solution 51

5.4.5 Relation between Sherwood Numbers and (Re.Sc) 60

CHAPTER 6 CONCLUSION AND RECOMMENDATION 66

REFERENCES 67

APPENDIX-A 72

VITAE 88

LIST OF TABLES

Table 1 summary to empirical correlations that were obtained for Newtonian solution.. 13

Table 2 summary to empirical correlations that were obtained for non-Newtonian solution..... 16

Table 3 Parameters of the experiments..... 21

Table 4 Parameters of linear polarization experiments..... 21

Table 5 Parameters of chronoampermetry experiments 22

Table 6 The power-law parameters..... 29

Table 7 Diffusivity of ferricyanide in free solution (0% CMC) 36

Table 8 Diffusivity of ferricyanide in 1% CMC solution..... 36

Table 9 Diffusivity of ferricyanide in 2% CMC solution..... 36

Table 10 Diffusivity of ferricyanide in 3% CMC solution..... 37

Table 11 Diffusivity of ferricyanide in 5% CMC solution..... 37

Table 12 the value of the slope, intercept, power index and consistency factor for all the solution..... 65

LIST OF FIGURES

Figure 1 Comparison of Prhashanna and Chhabra results with literature values [45]..... 12

Figure 2 Typical polarization curve obtained by the cyclic voltammetry method 18

Figure 3 Typical chronoampermetric curve..... 18

Figure 4 Experimental set-up illustration 23

Figure 5 Photograph of the experimental setup 24

Figure 6 Concentric cylinder viscometer..... 29

Figure 7 Viscosity vs. shear rate for 1% CMC solution 30

Figure 8 Viscosity vs. shear rate for 2% CMC solution 31

Figure 9 Viscosity vs. shear rate for 3% CMC solution 32

Figure 10 Viscosity vs. shear rate for 5% CMC solution 33

Figure 11 Typical chronampermetric curve to show the unsteady region..... 35

Figure 12 a typical graph of current vs.1/ (t) 0.5 35

Figure 13 polarization curve for spheres in free solution 40

Figure 14 Mass transfer coefficient vs. sphere diameter in solution without CMC 43

Figure 15 Mass transfer coefficient vs. sphere diameter at different speeds in solution without CMC 44

Figure 16 Mass transfer coefficient vs. sphere speed for different diameter in solution without CMC 45

Figure 17 Sherwood number vs. Reynolds number for different sphere in solution without CMC..... 46

Figure 18 Comparison of Sherwood Number vs. $Re^{1/2}$ $Sc^{1/3}$ in free solution 47

Figure 19 Polarization curve for 0.5cm sphere 5% CMC solution..... 49
Figure 20 Mass transfer coefficient vs. sphere diameter in non-Newtonian solution 50
Figure 21 Mass transfer coefficient vs. sphere speed for different diameter in 1% CMC solution..... 52
Figure 22 Mass transfer coefficient vs. sphere speed for different diameter in 2% CMC solution..... 53
Figure 23 Mass transfer coefficient vs. sphere speed for different diameter in 3% CMC solution..... 54
Figure 24 Mass transfer coefficient vs. sphere speed for different diameter in 5% CMC solution..... 55
Figure 25 Mass transfer coefficient vs. sphere speed for 1.0 cm sphere in different solutions 56
Figure 26 Mass transfer coefficient vs. sphere speed for 1.5 cm sphere in different solutions 57
Figure 27 Mass transfer coefficient vs. sphere speed for 2.0 cm sphere in different solutions 58
Figure 28 Mass transfer coefficient vs. sphere speed for 2.5 cm sphere in different solutions 59
Figure 29 Sherwood number (Sh) vs. $Re^{1/2}Sc^{1/3}$ for 1% CMC solution 61
Figure 30 Sherwood number (Sh) vs. $Re^{1/2}Sc^{1/3}$ for 2% CMC solution 62
Figure 31 Sherwood number (Sh) vs. $Re^{1/2}Sc^{1/3}$ for 3% CMC solution 63
Figure 32 Sherwood number (Sh) vs. $Re^{1/2}Sc^{1/3}$ for 5% CMC solution 64

LIST OF ABBREVIATIONS

A	:	Mass transfer area (cm^2)
F	:	Faraday's constant (C/mol)
D	:	Effective diffusivity (cm^2/s)
d	:	Diameter of sphere (cm)
C_b and C_s	:	The electrolyte Concentration at the bulk and the surface (mol/L)
n	:	Charge number of species
Ra	:	Rayleigh number
Gr	:	Grashof number
Nu	:	Nusselt number
Pr	:	Prandtl number
Sh	:	Sherwood numbe (k d / D)
Sc	:	Schmit number (ν / D)
Re	:	Reynolds number (ω d /ν)
n	:	Power index
K	:	Consistency factor (pa s^n)
k_L	:	Mass transfer coefficient (cm/s)
I_L	:	Limiting diffusion current (mA)
N_i	:	ion flux (mol/cm^2)
V	:	Potential (mV)

Greek Letters

μ	:	Dynamic viscosity (g cm/s)
ν	:	Kinematic viscosity (m^2/s)
ρ	:	Density at surface (g/cm^3)

ABSTRACT

Full Name : ABDULLAH MOHSIN BADURAIG

Thesis Title : SOLID-LIQUID MASS TRANSFER FROM SPINNING SPHERE IN NON-NEWTONIAN LIQUID

Major Field : MASTER OF SCIENCE IN CHEMICAL ENGINEERING

Date of Degree : MAY 3013

Mass transfer coefficients from spinning sphere in Newtonian and non-Newtonian solution have been experimentally obtained using electrochemical method called limiting diffusion current technique (LDCT). The effects of rotational velocity of the sphere, the size and the percent of CMC (carbxymethyl cellulose) in the solution were studied. Power index (n) and consistency factor (k) of the solution were obtained by measuring the stress of the solution at different shear rate using concentric cylinder viscometer. The diffusion coefficient of ferricyanide in sodium hydroxide was experimentally found from a method mentioned earlier by Noordsij. Average Sherwood numbers were calculated and data were compared with existing mathematical models. For Newtonian fluid, good agreement between the data obtained in this study and the one proposed by Noordsij was noticed for the Newtonian solution. The results of the experiments with different loading of CMC suggest that Sherwood number (Sh) is proportional to $Re^{1/2}$ $Sc^{1/3}$, in which Re and Sc are Reynolds and Schmidt numbers, respectively.

ملخص الرسالة

الاسم الكامل: عبدالله محسن مبارك بادريق.

عنوان الرسالة: إنتقال الكتلة من الاجسام الكروية الصلبة في حالة الدوران الى السائل اللزج (الغير نيوتوني) المحيط بها.

التخصص: ماجستير في الهندسة الكيميائية.

تاريخ الدرجة العلمية: مايو ٢٠١٣م.

تم قياس معامل إنتقال الكتلة من الاجسام الكروية الصلبة في حالة الدوران الى السائل اللزج (الغير نيوتوني) المحيط بها وذلك بإجراء عدة تجارب. وقد تم اجراء التجارب باستخدام طريقة كهروكيميائية يطلق عليها تقنية تيار الإنتشار المحدود (LDCT). درس في هذا البحث تاثيير سرعة دوران الاجسام الكروية وأحجامها و كمية المادة اللزجة في المحلول على معامل إنتقال الكتلة في الاجسام الكروية. الدليل الأسي (n) و معامل الاقتران (k) للمحلول حصل عليها بواسطة قياس القوة الموثرة في السطح عند تحريك الجسم بسرعات معينة وقد استخدم جهاز الاسطوانات المتداخلة لقياس اللزوجة في ذلك. معامل الإنتقال الجزيئي اوجدت بطريقة نشرت في بحث سابق بواسطة الباحث نردوش. تم حساب رقم شيروود (Sh) في هذه البحث وتم مقارنة القيم المحسوبة مع المعادلات الرياضية المنشورة في الابحاث السابقة. طابقت نتائج هذا البحث نتائج نشرت من قبل في بحث نشر للبحاث نردوش وكانت مقاربة لها. النتائج التي حصل عليها في هذا البحث اقترحت وجود علاقة لرقم شروود Sh مع $Re^{1/2}\ Sc^{1/3}$ حيث ان Re هو رقم رنولد و Sc هو رقم شمت بالتتالي.

CHAPTER 1

INTRODUCTION

The increasing emergence of non-Newtonian fluids, such as molten plastics, drilling mud, emulsion, etc. as important materials and products in a large variety of industrial processes has stimulated a considerable amount of interest in the behavior of such fluids when in motion. In particular what has been studied most intensely for obvious practical reasons is how mass and heat are transferred to non-Newtonian fluid under the more common flow configuration usually met in practice.

The transfer of heat/mass from different shapes, such as sphere, cylinder, vertical plate, etc. submerge in Newtonian or non-Newtonain fluids has attracted attention of numerous researcher over the past years [1-46]. Studying of such shapes simulate many cases in life. Mainly, there are two experimental methods used to study the heat/mass transfer from solid bodies. The first method is by studying the rate of dissolution of benzoic acid in the solution which was used by Donatelli and hyde [43]. The second method is by utilizing the electrochemical limiting diffusion current technique. The heat transfer coefficient can be obtained through the analogy.

The electrochemical limiting diffusion current technique (LDCT) of mass transfer measurement is attractive method for evaluating the mass/heat transfer coefficient since the measurements are usually simpler, speedier and more accurate than direct measurements. Moreover, it is also easy to determine the heat/mass transfer performance

of the individual surfaces in a complex multi-surface geometry by isolating unwanted surfaces. Detailed description of LDCT is given in this next section.

This work is aimed at obtaining mass transfer coefficients from spinning sphere with different sizes and speeds in non- Newtonian fluid. The obtained data will be used to deduce empirical models for Sherwood numbers of these situations.

1.1 Motivation

An inspection survey of the literature showed that data from rotating sphere in non-Newtonian fluids appear to be absent. So, it is worthwhile to have this data available in the literate. Furthermore, many applications have been attributed to this case. An important application that can be simulated by this study is the rotating of drilling bit in the petroleum industry. Another case can be found in the steel industry when holes are required to be made in steel to make it in certain shapes. Also, in a stirred vessel the movement of a particle is basically a combination of rotation and translation. More engineering applications can be simulated by this study such as projectile motion, fiber coating and so on.

1.2 Research Objective

The following are the specific objectives of the present thesis work:

i. Obtaining the mass transfer coefficients by using LDCT from spinning spheres in non-Newtonion liquids.

ii. To investigate the effect of the following parameters on the mass transfer coefficient:

    a. Loading of CMC (carbxymethyl cellulose)

    b. Angular velocity

    c. Size of the sphere

CHAPTER 2

LITERATURE REVIEW

2.1 Limiting Diffusion Current Technique (LDCT)

The electrochemical method is based on a diffusion-controlled reaction at the electrode surface and mass transfer between electrode surface and electrolyte solution. When an electric potential is applied between two electrodes in an aqueous solution of an electrolyte an ionic reduction occurs at the cathode and an oxidation at the anode. As a result, a current which is proportional to the number of ions reacting at the electrodes per unit time, flows through the circuit [1]. When the potential on the electrode is gradually increased the current first increases until a stable value is reached. This value is called the limiting current and it corresponds to the condition when the concentration of the reacting species of ions on the surface of the electrode equals zero. At steady state, ions that are converted at the electrode have to be supplied from the bulk of the liquid [1]. This can occur by a diffusion process under the effect of the concentration gradient and by migration of the ions in the electric field. To suppress the last effect or make it negligible compared to diffusion and convection, a high concentration of inert electrolyte is used. In the electrochemical method during the transport of substance and charge in the electrolyte stream, ions from the main mass solution are transferred to the surface of the electrode. The overall rate of reaction (that includes mass transfer) becomes mass transfer limited as

the rate of reaction becomes very fast [1]. The rate of the reaction can now be derived as follow:

- By Faraday's law the current density i (I_L/A) is proportional to the reacting ion (or molecule) flux N_A:

$$I_L = -AnFN_i \quad or \quad N_i = \frac{I_L}{AnF} \tag{2.1}$$

Where,

I_L = the limiting current (mA)

A = Area of the electrode (cm^2)

n = charge number of the species

F = Faraday's constant (c/mol)

- The deriving of the mass-transfer process now can be related to concentration gradient of the reacting species. As result, Mass-transfer rates then can be related in general way to the concentration driving force:

$$N_A = k_L(C_b - C_s) \tag{2.2}$$

Where,

k_L = Mass transfer coefficient (cm/s)

C_b and C_s are the electrolyte concentrations at the bulk and the surface, respectively (mol/cm^3).

By equating (2.1) & (2.2) the following equation will be obtained

$$N_A = k_L(C_b - C_s) = \frac{I_L}{AzF} \tag{2.3}$$

At the limiting condition, the concentration of the electrolyte at the surface is approximately zero. Then equation (2.3) becomes

$$k_L = \frac{I_L}{A\ z\ F\ C_b} \tag{2.4}$$

Equation (2.4) is used to calculate mass transfer coefficient at any surface for a given situation.

There to many systems are available for reaction used in electrochemical mass transfer studied. The following are the most one used

Cathodic:

$$Cu^{2+} + 2e \longrightarrow Cu$$

$$Fe(CN)_6^{3-} + e \longrightarrow Fe(CN)_6^{4-}$$

Anodic:

$$Fe(CN)_6^{4-} \longrightarrow Fe(CN)_6^{3-} + e$$

Also in chemical engineering this method has been used, for example: in the studies of pulsate and oscillate flows between parallel plate (plate heat exchanger) [2–5], in evaluation of the thickness of boundary convection mass transfer [6–8], in the measurement of liquid film thickness in Newtonian [9] and

non-Newtonian fluids [10], in pipes flow [11–14], in packed column [15,16], in fluidization processes [17,17] and membrane reactor [19].layer in natural

2.2 Mass Transfer Coefficient from Sphere

2.2.1 Newtonian Fluid

Owing to its fundamental significance, considerable research efforts have been expended in studying free convection heat/mass transfer from a sphere in Newtonian fluids, typically air or water. Early analytical attempts employ either the boundary layer flow approximation (large values of Grashof number), or rely on the applicability of matched asymptotic expansion method in the other limit of vanishingly small values of Grashof number. Obviously, the boundary layer approximation breaks down in the wake region of the sphere. The utility of boundary layer approach is exemplified by the studies of Merk and Prins [20], Chiang et al. [21], Stewart [22] and Potter and Riley [23] and others (Jafarpur and Yovanovich, [24]). On the other hand, the small Grashof number case has been tackled amongst others by Fendell [25], Singh and Hasan [26], etc. Only over the past 15–20 years, numerical solutions to the complete governing equations have been sought. Geoola and Cornish [27] were seemingly the first to provide completely numerical solutions for free convection from a sphere in air (Pr=0.72) over the range of Grashof number as: $0.05 \leq Gr \leq 50$. They reported extensive results on drag coefficient and Nusselt number, the latter were shown to be in fair agreement with the experimental results. However, their numerical scheme failed to converge for $Gr>50$. Subsequently,

they (Geoola and Cornish, [28]) extended this work to elucidate the role of Prandtl number on the flow and heat transfer Characteristics in the free convection regime by considering additional values of Prandtl number (Pr=10 and100).They circumvented the convergence difficulties by seeking solutions to time- dependent equations. Subsequently, Farouk [29] reported numerical results on local and mean Nusselt numbers over the range of Rayleigh number (Ra=Gr×Pr) $10^{-1} \leq Ra \leq 10^4$. Both Fujii et al. [30] and Riley [31] provided time-dependent solutions for the free convection regime. For Pr=0.72 (air) and Ra=100, Fujii et al. [30] showed that it was sufficient to use the outer boundary of radius of 40 times that of the sphere as far as the value of the steady state average Nusselt number is concerned. They also noted that while their values of the average Nusselt number were within 72% of those based on the boundary layer approximation, but the two results differ significantly at the stagnation points. Similarly, Riley (1986) solved the time-dependent equations for Pr=0.72 and 7 and for Gr=500 and 10^4 and he reported the evolution of Nusselt number with time. His results are also consistent with the other predictions available in the literature [23]. Subsequently, Takamatsu et al. [32] have revisited this flow and elucidated the influence of domain size and Prandtl number on the free convection from a sphere in fluids with $0.7 \leq Pr \leq 120$. Their results suggest that larger domains are needed with the increasing value of the Rayleigh number in order to obtain the results which are largely free from domain effects. Thus, for Pr=0.7 and Ra=1, they suggest a spherical domain $(D_\infty/D) \geq 60$ to be adequate. Dudek et al. [33] have estimated the drag force on a sphere induced by buoyancy currents which were found to be in good agreement with their simulations. Their results, however, relate to extremely small values of the Grashof number, $0.002 \leq Gr \leq 0.3$ in air. Johnson et al. [34] also

reported numerical results for free convection from a sphere in air which are in line with the previous numerical and experimental results available in the literature. In recent years, there has been a renewed interest in studying free convection from a sphere in Newtonian fluids [35, 36 and 37]. Jia and Gogos [35, 36] have reported numerical results on free convection from isothermal spheres in air over extended range of Grashof number, $10 \leq Gr \leq 10^8$, using both steady and transient simulations. The effect of Prandtl number has been studied extensively by Yang et al. [37].

The above-mentioned numerical Advances have been supplemented by a few experimental studies on free convection from a sphere. Amato and Tien [38] studied the laminar free convection heat transfer from sphere to water over wide range of Rayleigh number.

2.2.2 Non-Newtonian Fluid

In contrast, much less work is available for heat transfer from a sphere in power law fluids. Early studied on laminar natural convection heat transfer was performed by the pioneer Acrivos [39]. His study was based on the boundary layer flow approximation and specified for Pr>10. Subsequently, Stewart [22] revisted the Acrivos problem and gave numerical solution for the same study of Acrivos. Finite values of Prandtl and Grashof number were allowed in Stewart solution.

On the other hand, only Liew and Adelman [40] have reported Experimental results on free convection from a heated sphere in power-law fluids. Over the range of conditions,

$0.3 < n < 1$ and $8.8 \times 10^5 \leq Ra \leq 3.4 \times 10^8$, they reported their mean values of the Nusselt number to be in fair agreement with the predictions of Acrivos [39] and they also put forward an empirical correlation.

Amato and Tien [41] extended their previous study with water to free convection from a heated sphere in power-law fluids using Polymer solutions. They presented extensive temperature profiles and Nusselt number data which were broadly in line with the results of Acrivos [39]. Further study was done by Churchill [42] proposed an equation that will cover the entire range for $Gr<10^9$. The numerator of the discovered equation represents the same correlation obtained by Stewart [22] and the denominator approaches unity because pseudoplastic fluids have a very large Schmidt number.

Furthermore, Lee and Donatelli [43] studied the mass transfer behavior from solid spheres of benzoic acid to non-newtonain fluids, consisting of various types of carboxymethyl cellulose solution. The results were compared to the theoretical models that discovered from previous studies. The correlation equation proposed by Churchill [44] appeared to be able to predict the mass-transfer behavior over the entire laminar region and assumed to applicable for both Newtonian and power law fluids.

Recently, theoretical study of free convection in power law fluid from a heated sphere was carried out by Prhashanna and Chhabra [45] .In this study, Consideration has been given to elucidate the role of Grashof number (Gr), Prandtl number (Pr) and power-law index(n), on the value of the Nusselt number(Nu) for a sphere in the natural convection regime. The results from this study encompass the following range of conditions: $0.4 \leq n \leq 1.8$; $10 < Gr < 10^7$ and $0.72 < Pr < 100$.The agreement between the numerical results

and the prediction correlations by the previous studies are seen to be satisfactory. The following figure shows comparison between Chhabra and the other.

Finally, one more study on the porous medium in power law fluid was considered early by Han-Taw chen and Cha'o-Kuang chen [46]. This study was based on the boundary layer approximation and only suitable for a high Rayleigh number.

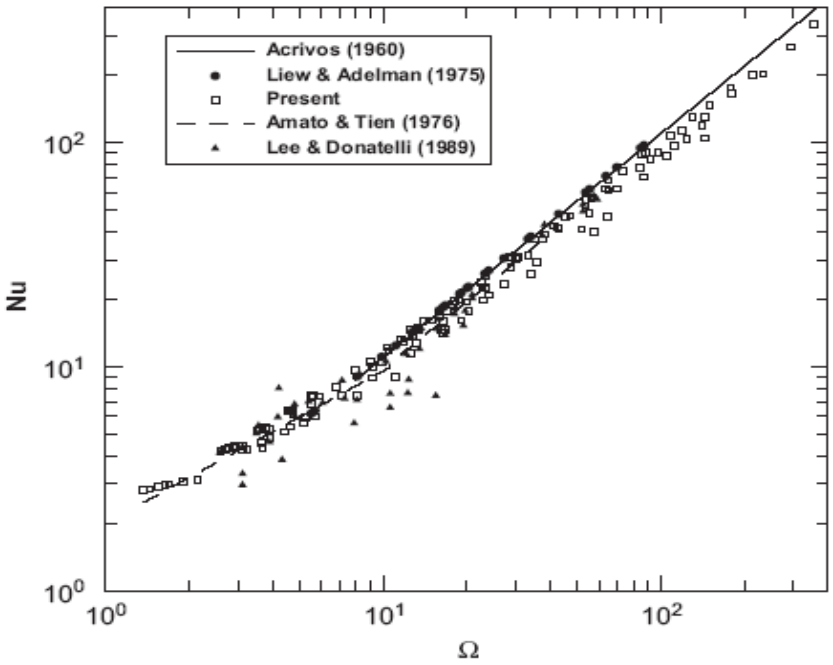

Figure 1 Comparison of Prhashanna and Chhabra results with literature values [45].

.

Table 1 summary to empirical correlations that were obtained for Newtonian solution

	Authors	Empirical Correlation	Limitations	Comment
1	Acrivos (1960)	$Sh = C\ Gr^{\frac{1}{2(n+1)}} Sc^{\frac{n}{3n+1}}$	-Based on boundary layer approximation and for Pr>10 -C ranges from 0.9 for n=0.1 and 1.4 for n=1.5. Acrivoe suggested the use of a mean value of C=1.1	Numerical
2	Stewart (1971)	$Sh = C\ (Gr\ Sc)^{\frac{1}{3n+1}}$	It covers wide range of Pr and Gr numbers	Numerical
3	Liew and Adelman (1975)	$Sh = 1.122\ Gr^{\frac{1}{2n+1}} Sc^{\frac{n}{3n+1}}$	Applicable for - $0.66 \le n \le 1$ - $8x10^2 \le Ra \le 1.3\ x10^8$	Experimental (copper spheres)
4	Amato and Tien (1976)	$Sh = \Omega$ for $\Omega > 10$ $Sh = 2\ \Omega^{0.682}$ for $\Omega < 10$	$\Omega = Gr^{\frac{1}{2(n+1)}} Sc^{\frac{n}{3n+1}}$ Applicable for - $1.5 \le Nu \le 20$ - $0.6 \le n \le 0.95$	Experimental
5	Churchill (1983)	$Sh = 2 + \frac{0.589(Gr\ Sc)^{\frac{1}{3n+1}}}{\left[1+\left(\frac{0.43}{Sc}\right)^{\frac{9}{16}}\right]^{\frac{4}{9}}}$	$Gr<10^9$ Applicable for both Newtonain and power law fluid	Numerical
6	Prhashanna and Chhabra (2010)	$Sh = \Omega$ for $\Omega > 10$ $Sh = 2\ \Omega^{0.72}$ for $\Omega < 10$	$\Omega = Gr^{\frac{1}{2(n+1)}} Sc^{\frac{n}{3n+1}}$ - $0.4 \le n \le 1.8$ - $10 < Gr < 10^7$ - $0.72 < Sc < 100$	Numerical

2.3 Mass Transfer Coefficient from spinning sphere

2.3.1 Newtonian Fluid

The problems occurring in convective heat transfer over a heated rotating sphere have been the concern of researchers and engineers for more than 150 years [47-52]. Many authors concentrated on determining the average Nusselt number (Nu) of the rotating sphere an important parameter in describing the heat transfer characteristics, as well as the formulas of Nu correlating other physical parameters in different operating ranges. For instance, in free convection dominated flow, Yuge [53] experimentally measured Nu and obtained an empirical equation correlating Nu with the Grashof number (Gr). By assuming the flow around the sphere was laminar, Dorfman and Serazetdinov [54] theoretically determined a relation for Nu of a rotating sphere in the forced convection region

$$Nu = 0.33\ Re^{0.5}\ Pr^{0.4} \tag{2.5}$$

Kreith et al. [55] correlated their experimental data by a similar relation to that of equation (2.5), but with a larger coefficient (0.43). This discrepancy in the coefficient may be due to the fact that Dorfman and Serazetdinov [54], in their theoretical analysis, neglected the effect of the eruption jet near the equatorial plane observed by Kreith et al. using smokevisualization [55]. Banks [56], assuming the flow around the spinning sphere to be entirely laminar from the pole to the equator, obtained a correlation by numerical calculation of the same form but with a coefficient of 0.26, for Pr = 0.7. For large

rotational Reynolds number (5 x 10’ < Re < 7 x 106), the experimental results of Kreith et al. [55] were found to be correlated within a deviation of about 15% by the relation

$$Nu=0.066Re^{0.67}Pr^{0.4} \quad (2.6)$$

Tieng and Yan [57] measured the average Nusselt number of a heated sphere rotating in quiescent air was measured experimentally over the range 0 < Re < 33320 from free to force convection regimes.

Noordsij and Rotte [58] developed model for rotating and vibrating sphere with an electrochemical method. The results of the experiments suggest that Sherwood number is proportional to $Re^{1/2}Sc^{1/3}$. The following relation represents the relation ship

$$Sh=10+0.43\ Re^{1/2}Sc^{1/3} \quad (2.7)$$

the above equation covers the following ranges

$$0.8\times10^3 < Re < 27\times10^3$$

And

$$0.5\times10^3 < Sc < 2\times10^3$$

Table 2 summary to empirical correlations that were obtained for non-Newtonian solution

	Authors	Empirical Correlation	Limitations	Comment
1	Dorfman and Serazetdinov	$Nu = 0.33\ Re^{0.5} Pr^{0.4}$	- assuming the flow around the spinning sphere to be entirely laminar	Numerical
2	Kreith et al.	$Nu=0.066Re^{0.67}Pr^{0.4}$	Large Reynolds number $5 \times 10^{5} < Re < 7 \times 10^{6}$	Experimental
3	Noordsij and Rotte	$Sh=10+0.43\ Re^{1/2}Sc^{1/3}$	Applicable for $- 0.8\times10^{3} < Re < 27\times10^{3}$ $- 0.5\times10^{3} < Sc < 2\times10^{3}$	Experimental

2.4 Electrochemical Method

2.4.1 Cyclic Voltammetry

Cyclic voltammetry (CV) is the most widely used technique for acquiring qualitative information about electrochemical reactions. CV provides information on redox processes, heterogeneous electron-transfer reactions and adsorption processes. It offers a rapid location of redox potential of the electoactive species.

CV consists of scanning linearly the potential of a stationary working electrode using a triangular potential waveform. During the potential sweep, the potentiosatat measures the current resulting from electrochemical reactions (consecutive to the applied potential). The cyclic voltammogram is a current response as a function of the applied potential. Figure 2 shows typical polarization curve obtained by cyclic voltammetry method.

2.4.2 Choronoamperometry

The basis of the controlled-potential techniques is the measurement of the current response to an applied potential step. Choronoamperometry involves stepping the potential of the working electrode from an initial potential, at which (generally) no faradic reaction occurs, to a potential E_i at which no electroactive species exist (at the beginning of the experiment). The current-time response reflects the change in the concentration gradient in the vicinity of the surface species or the surface area of the working electrode. The typical choronoamperometric curve is shown in Figure 3.

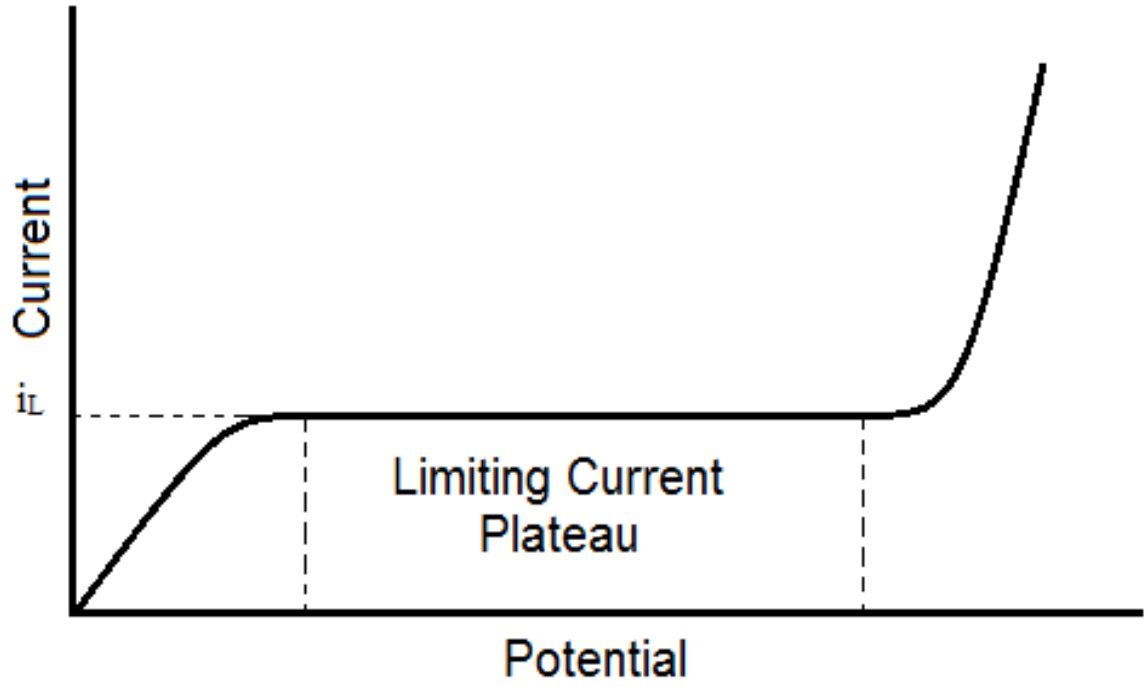

Figure 2 Typical polarization curve obtained by the cyclic voltammetry method

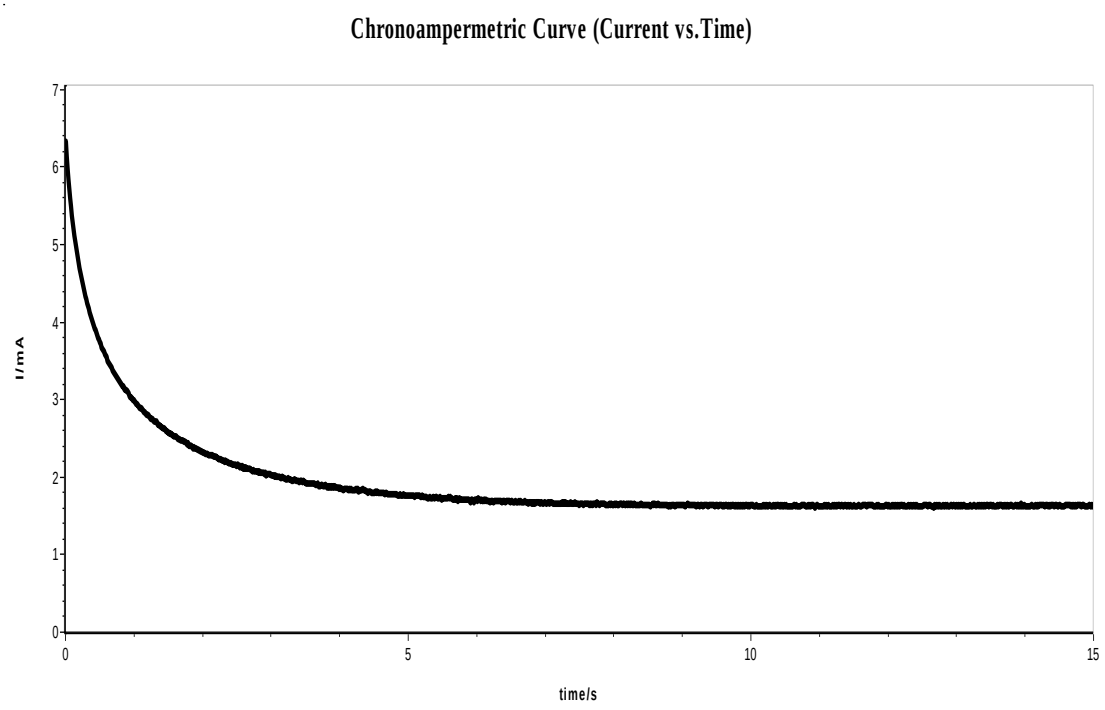

Figure 3 Typical chronoampermetric curve

CHAPTER 3

EXPERIMENTAL SET-UP AND METHODOLOGY

3.1 The Experimental Set-Up

The experimental set-up for this study is shown in Fig.4. Ferri-ferrocyanide in sodium hydroxide was chosen to estimate the limiting diffusion current. This system was selected due to it is well-defined limiting current plateau and the solubility of CMC (carbxymethyl cellulose) in the solution. A 500 ml equimolar solution of 0.0092 M ferricyanide ($Fe(CN)_6^{3-}$), ferrocyanide ($Fe(CN)_6^{4-}$) and 0.5 M of sodium hydroxide NaOH was prepared in a vessel. Four more solutions with different percent of CMC, namely; 1.0%, 2.0%, 3.0% and 5.0% were prepared with the same concentration of ferri-ferrocyanide and NaOH.

Four stainless steel spheres of 1.0, 1.5, 2.0 and 2.5 cm diameter were fabricated from commercial stainless steel block. A thin stainless steel rod was welded on each sphere for electrical connection. The surfaces of these spheres were masked with an insulating paste such as to deactivate the unwanted area. The prepared assembly was embedded in the prepared solution to act as working electrode .A stainless steel cylinder, kept inside the vessel, near to the wall, worked as counter electrode. A saturated calomel electrode was embedded in the solution to function as reference electrode. The working electrode was connected to motor to rotate the spheres and the rotational speed was controlled manually

by adjusting the knob on the desired speed. All the parameters that were varied during the experiment are shown in Table 3.

The temperature of the solutions was measured by a thermometer. The working, counter and reference electrodes were connected to potentiostat (Model MPG2, Bio Logic). The potentiostat MPG2 was driven by a manufacturer software package a EC-Lab software version 10.19 via a computer. Potentiostatic linear polarization and chronoampermetric curves were obtained for samples spheres embedded in different solution (Appendix A). The electrochemical parameters maintained during the experiments are listed in Table 4 and Table 5. Figure 4 and Figure 5 show the photographs of the experimental set-up and the electrochemical cell.

The data were acquired at room temperature 25^{o}C which remained almost constant during an experiment but varied between different experiments. The temperatures were recorded accurately for each experiment.

Table 3 Parameters of the experiments

Concentration of ferri-ferrocyanide	0.0092 M	**Concentration of sodium hydroxide NaOH**	0.5 M

Speed Rad/s	0.0	3.54	7.83	14.69	22.13	29.74

% CMC	Pure	1.0%	2.0%	3.0%	5.0%

Sphere D	1.0cm	1.5 cm	2.0 cm	2.5 cm

Table 4 Parameters of linear polarization experiments

Parameter	**Value**	**Unit**
Conditioning Time	60	seconds
Initial Potential	200	mV SCE
Final Potential	750	mV SCE
Scan Rate (dV/dt)	0.5	mV/s
Reference Electrode	241.5	mV SCE

Table 5 Parameters of chronoampermetry experiments

Parameter	**Value**	**Unit**
Applied Potential	520	mV SCE
Scan rate (dI/dt)	0.50×10^{-6}	μA/s
Conditioning Time	200s-20s	seconds

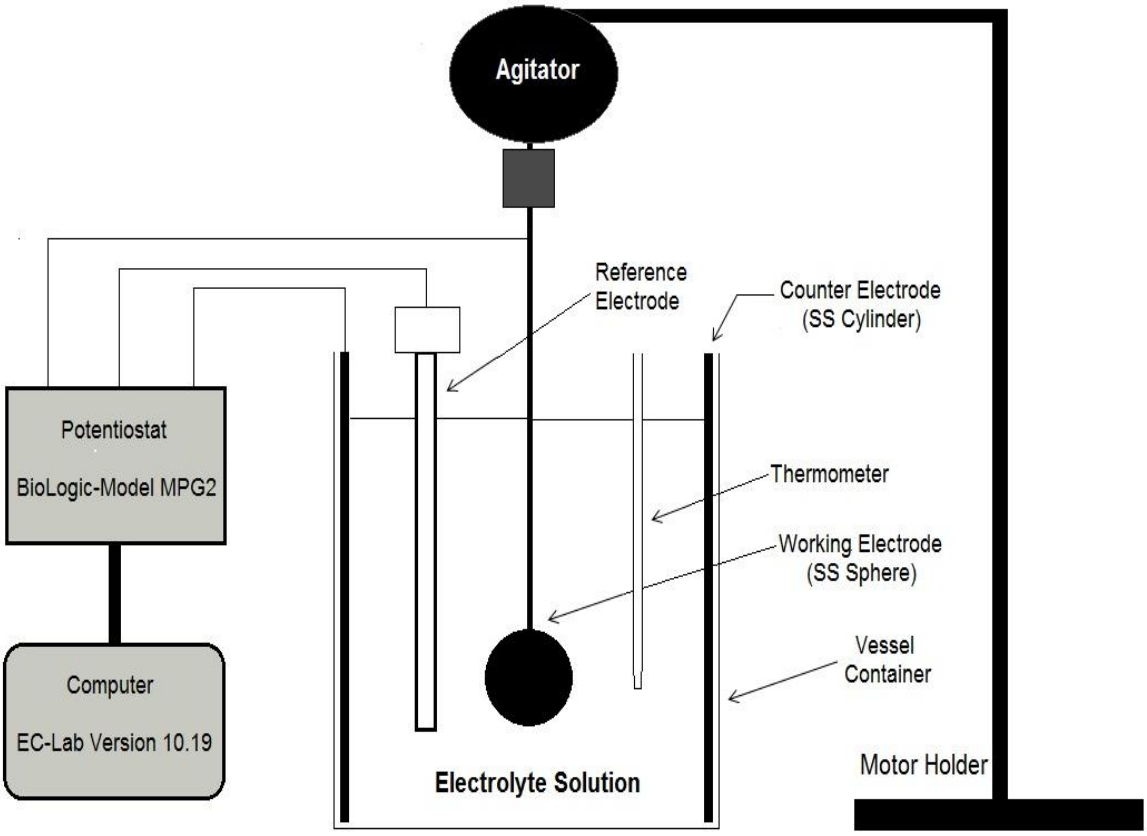

Figure 4 Experimental set-up illustration

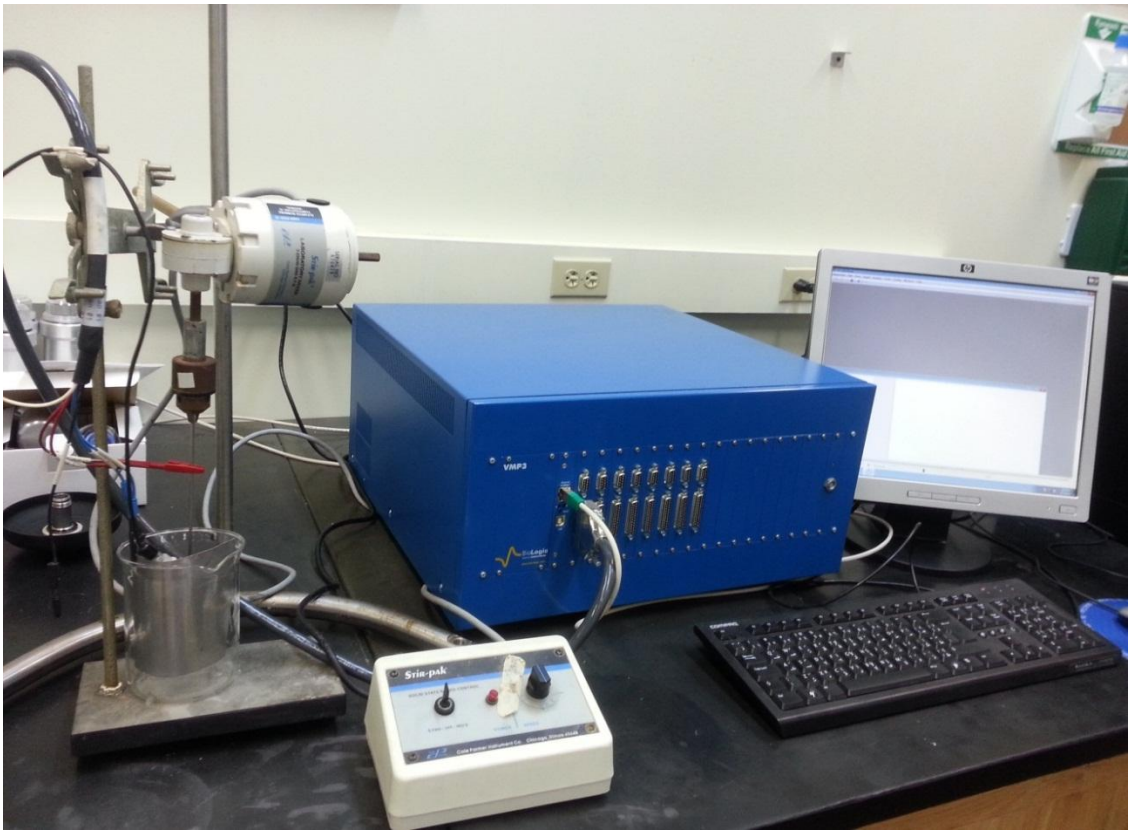

Figure 5 Photograph of the experimental setup

3.2 Methodology of Performing the Experiment

The following steps represent the procedure of how the experiment was carried out:

1. Preparation of the electrolyte solution (x M $Fe(CN)_6^{-3}$ + x M $Fe(CN)_6^{-4}$ + x M NaOH)

2. Set up the electrochemical cell that contained the following:

- Counter electrode (cylinder of stainless steel)

- Working electrode (sphere fabricated from stainless steel with different sizes)

- Supporting electrode to prevent the migration of ions such as NaOH.

3. Turn on the potentiostat and the computer.

4. Ran the program and choose the method that was used to get the linear polarization curve. In our case, the suitable method to be used was the cyclic voltammetry.

5. After I chose the correct method, the experiment parameters that were necessarily to start the test such as initial potential, final potential, scan rate etc.

6. From the polarization curve, the limiting diffusion current was obtained from the plateau.

7. The obtained value of the current was used to calculate the mass transfer coefficient from the equation mention before.

8. Rheological properties such as index factor (n) and consistency factor (k) were obtained by using viscometer device. More about the method will be included in the next chapter.

9. Physical properties of the solution evaluated from the available correlation in the literature.

CHAPTER 4

PHYSICAL PROPERTIES

4.1 Viscosity Measurement

Sodium carboxymethylcellulose is known by CMC or as a food grade product as cellulose gum. It is soluble in both hot and cold water. CMC are used as thickening, binding, stabilizing, and film-forming agents. CMC is water soluble material used in oil recovery and other applications.

Four different solutions were prepared each contained certain amount of CMC (1%, 2%, 3% and 5%).The rheological properties of the solutions were obtained by measuring shear stress as function of shear rate with concentric cylinder viscometer as shown Figure 6. It basically consists of two concentric cylinders and a small intervening annular space contains the test fluids whose viscosity is to be determined. The inner cylinder is rotated at a constant angular speed. The viscous drag due to the liquid between the cylinders produce a torque on the inner cylinder, which would rotate if it was not restrained by an equal and opposite torque. Steady shear rate was used to study the viscosity and the shear rate range was between 0.1-100 rad/s.

The results of the rheological measurements are given in Figure 7 through Figure 10. The viscosity of the solution decreases as the shear rate increases (shear thinning behavior).

From theses it can be seen that the liquids obey the power-law over the shear rate range considered. The values of the power-law parameters were calculated and are given in Table 6 .

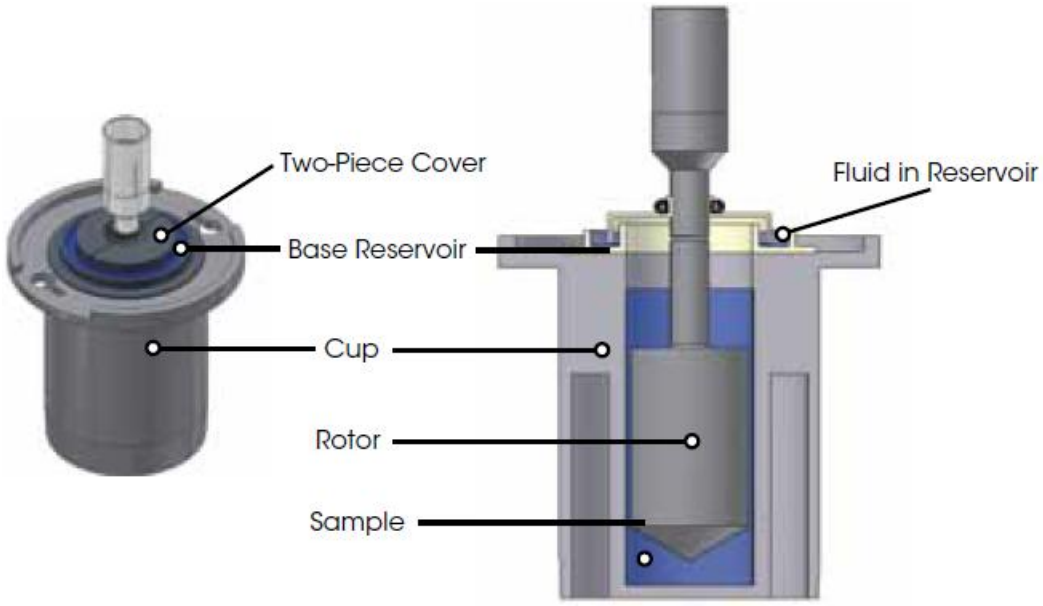

Figure 6 Concentric cylinder viscometer

Table 6 The power-law parameters

% of CMC	**n**	**K (Pa.s^n)**
1%	0.89	0.00743
2%	0.85	0.42
3%	0.777	1.59
5%	0.62	11.7

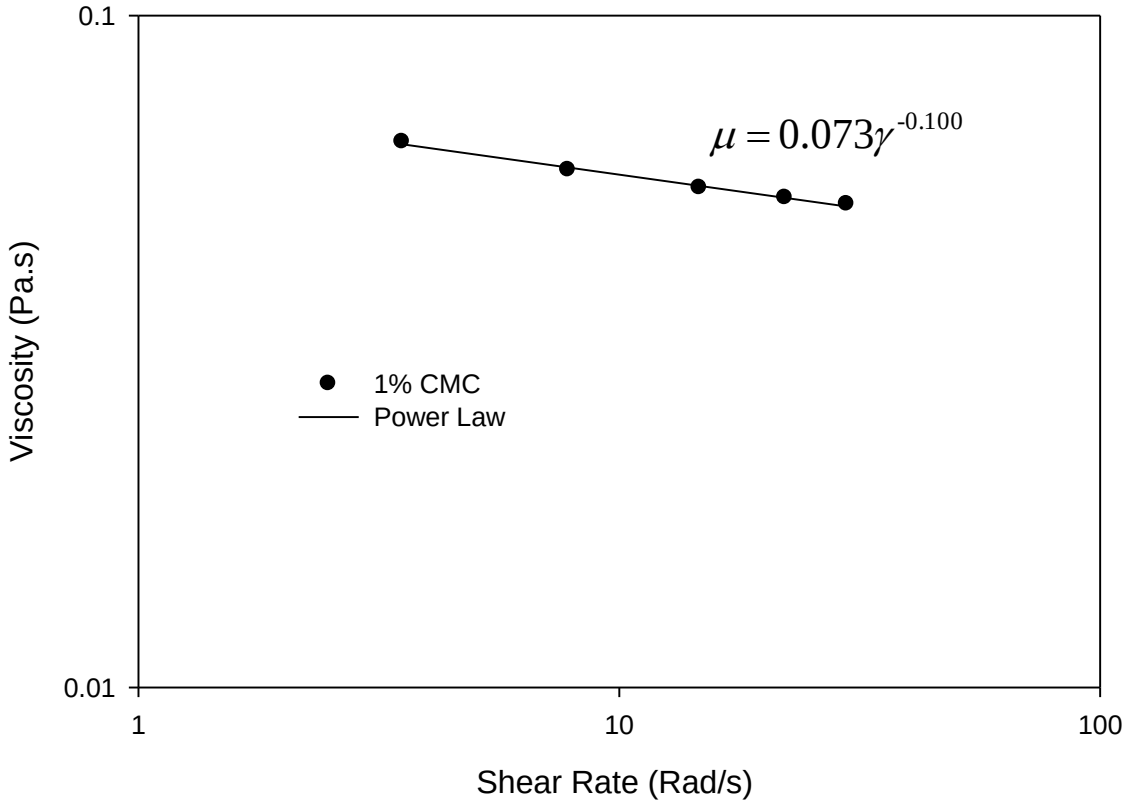

Figure 7 Viscosity vs. shear rate for 1% CMC solution

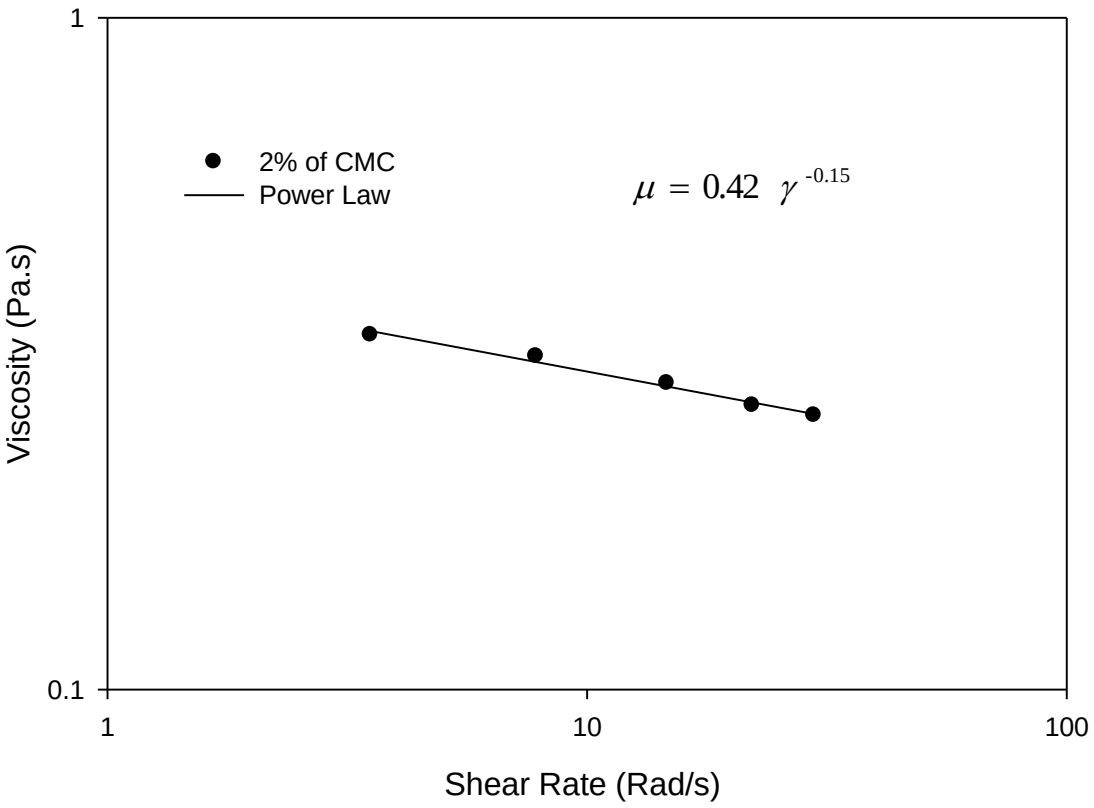

Figure 8 Viscosity vs. shear rate for 2% CMC solution

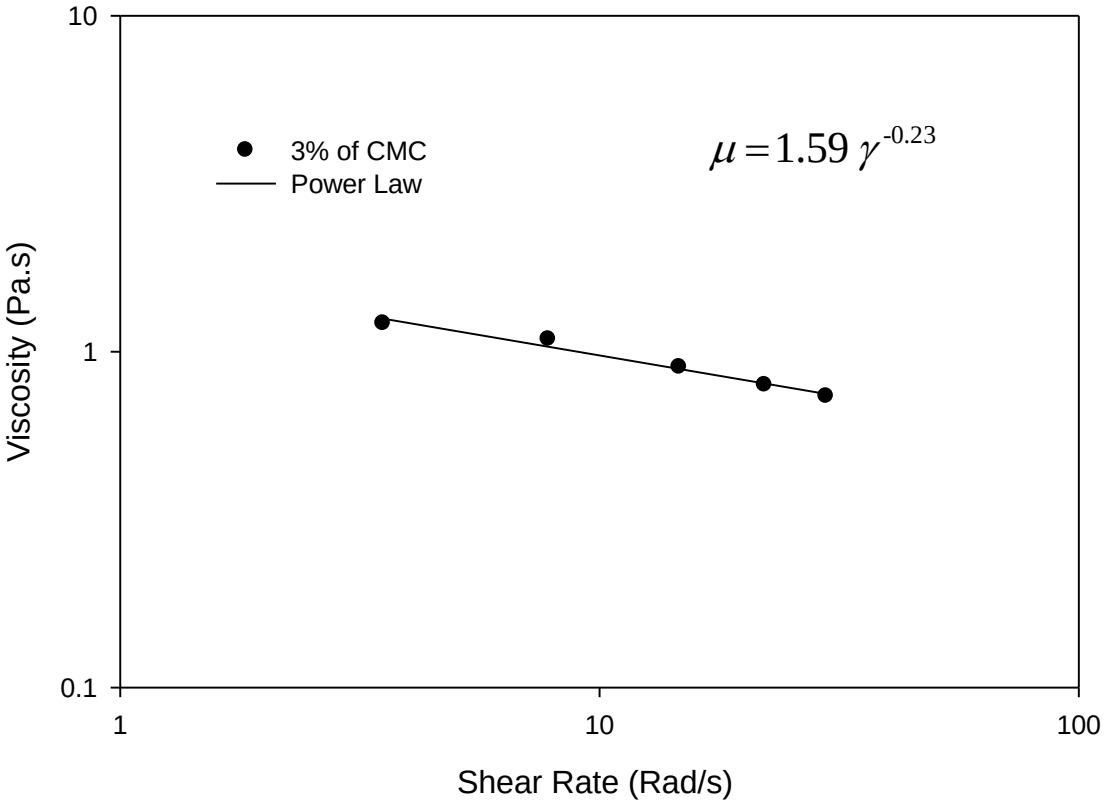

Figure 9 Viscosity vs. shear rate for 3% CMC solution

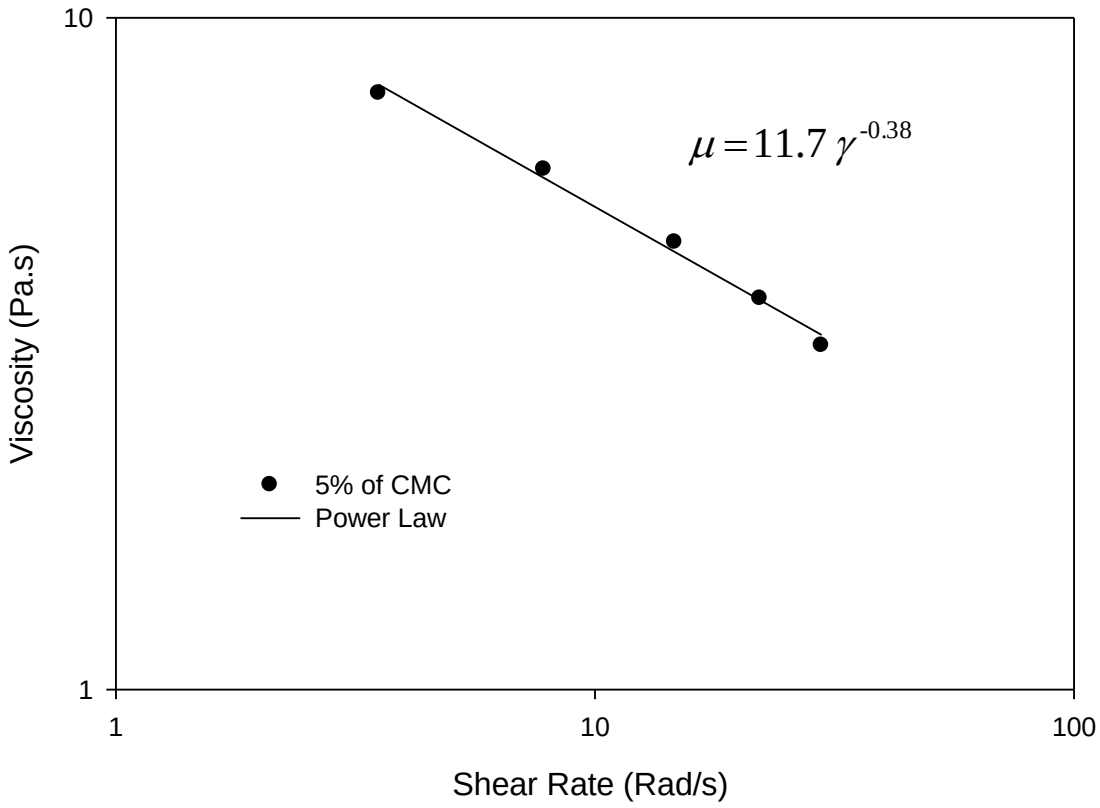

Figure 10 Viscosity vs. shear rate for 5% CMC solution

4.2 Diffusion Coefficient Measurement

The measurement of the diffusion coefficient was performed as Noordsij described earlier [58]. When constant potential was applied through the electrodes, the current starts to flow across the electrode. This causes rise to a great concentration gradient at the cathode and therefore ferriccyanide ions will move toward the spheres. After a short period during which chemical reaction on the cathode is rate controlling, the current can be describe by

$$i = F\ A < C > \left(\frac{2\ D}{d} + \sqrt{\frac{D}{\pi\ t}}\right) \tag{4.1}$$

The diffusion coefficients could then be deduced from record of current as a function of time. Figure 12 shows a typical graph of current vs.1/ $(t)^{0.5}$ at the unsteady period of the chronoampermetric curve Figure11.

The results of the diffusion coefficient for different experimentsp are tabulated in Table 7 through Table 11. From the results, it is noted that as the rotational speed of the spheres increases the diffusion coefficient increases and this can be attributed to the increasing of ions movement in the solution. As the percent of CMC in the solution increases, the diffusion coefficient decreases because of the resistant of ion to move in the solutions.

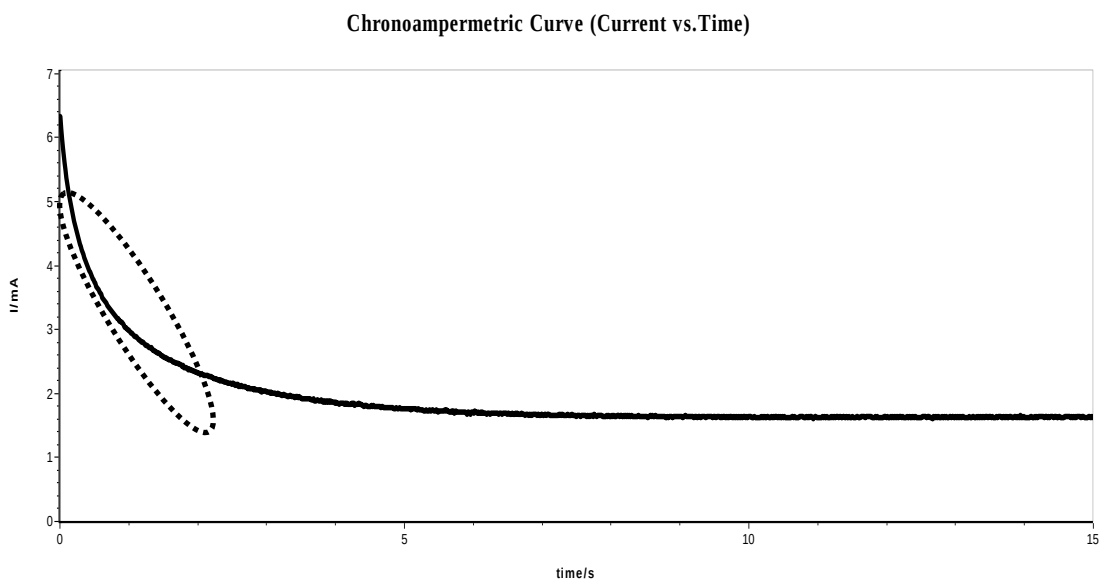

Figure 11 Typical chronampermetric curve to show the unsteady region

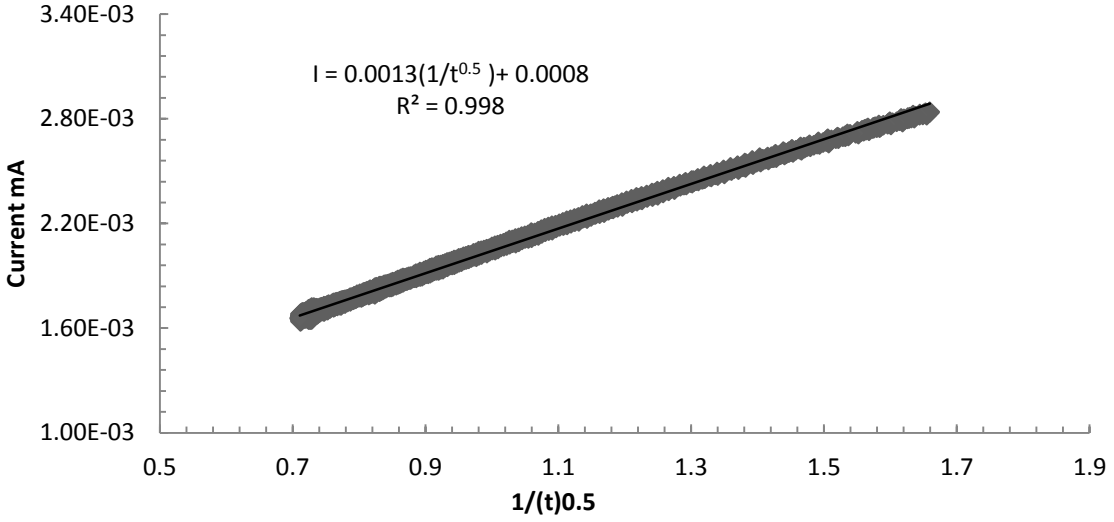

Figure 12 a typical graph of current vs.1/ (t) 0.5

Table 7 Diffusivity of ferricyanide in free solution (0% CMC)

	Diffusivity of Ferri-cyanide (m^2/s)				
Speed/Diameter	**0.5**	**1**	**1.5**	**2**	**2.5**
0.00	5.90E-10	5.90E-10	5.90E-10	5.90E-10	5.90E-10
3.54	5.90E-10	5.90E-10	5.90E-10	5.90E-10	5.90E-10
7.83	5.90E-10	5.90E-10	5.90E-10	5.90E-10	5.90E-10
14.69	5.90E-10	5.90E-10	5.90E-10	5.90E-10	5.90E-10
22.13	5.90E-10	5.90E-10	5.90E-10	5.90E-10	5.90E-10
29.74	5.90E-10	5.90E-10	5.90E-10	5.90E-10	5.90E-10

Table 8 Diffusivity of ferricyanide in 1% CMC solution

	Diffusivity of Ferri-cyanide (m^2/s)				
Speed/Diameter	**0.5**	**1**	**1.5**	**2**	**2.5**
0.00	5.33E-10	5.33E-10	5.33E-10	5.33E-10	5.33E-10
3.54	6.40E-10	6.40E-10	6.40E-10	6.40E-10	6.40E-10
7.83	7.04E-10	7.04E-10	7.04E-10	7.04E-10	7.04E-10
14.69	7.74E-10	7.74E-10	7.74E-10	7.74E-10	7.74E-10
22.13	8.51E-10	8.51E-10	8.51E-10	8.51E-10	8.51E-10
29.74	9.36E-10	9.36E-10	9.36E-10	9.36E-10	9.36E-10

Table 9 Diffusivity of ferricyanide in 2% CMC solution

	Diffusivity of Ferri-cyanide (m^2/s)				
Speed/Diameter	**0.5**	**1**	**1.5**	**2**	**2.5**
0.00	4.10E-10	4.10E-10	4.10E-10	4.10E-10	4.10E-10
3.54	4.92E-10	4.92E-10	4.92E-10	4.92E-10	4.92E-10
7.83	5.41E-10	5.41E-10	5.41E-10	5.41E-10	5.41E-10
14.69	5.95E-10	5.95E-10	5.95E-10	5.95E-10	5.95E-10
22.13	6.55E-10	6.55E-10	6.55E-10	6.55E-10	6.55E-10
29.74	7.20E-10	7.20E-10	7.20E-10	7.20E-10	7.20E-10

Table 10 Diffusivity of ferricyanide in 3% CMC solution

Diffusivity of Ferri-cyanide (m^2/s)					
Speed/Diameter	**0.5**	**1**	**1.5**	**2**	**2.5**
0.00	3.15E-10	3.15E-10	3.15E-10	3.15E-10	3.15E-10
3.54	3.78E-10	3.78E-10	3.78E-10	3.78E-10	3.78E-10
7.83	4.16E-10	4.16E-10	4.16E-10	4.16E-10	4.16E-10
14.69	4.99E-10	4.99E-10	4.99E-10	4.99E-10	4.99E-10
22.13	5.49E-10	5.49E-10	5.49E-10	5.49E-10	5.49E-10
29.74	6.04E-10	6.04E-10	6.04E-10	6.04E-10	6.04E-10

Table 11 Diffusivity of ferricyanide in 5% CMC solution

Diffusivity of Ferri-cyanide (m^2/s)					
Speed/Diameter	**0.5**	**1**	**1.5**	**2**	**2.5**
0	2.10E-10	2.10E-10	2.10E-10	2.10E-10	2.10E-10
33.8	2.52E-10	2.52E-10	2.52E-10	2.52E-10	2.52E-10
74.8	2.77E-10	2.77E-10	2.77E-10	2.77E-10	2.77E-10
140.3	3.05E-10	3.05E-10	3.05E-10	3.05E-10	3.05E-10
211.3	3.35E-10	3.35E-10	3.35E-10	3.35E-10	3.35E-10
284	3.69E-10	3.69E-10	3.69E-10	3.69E-10	3.69E-10

CHAPTER 5

RESULTS AND DISSCUSION

This chapter essentially has two main parts. The first one concerns about the Newtonian fluid in which the solution has constant viscosity (0% of CMC). The polarization curve is shown and the effects of varying the diameter, speed are discussed. After that, comparison between our result the one proposed by Nerdoosh was presented. The second part of the result is a bout the non-Newtonian fluid in which considerable amount of CMC% was added to increase the viscosity of the solution. The effect of varying the spheres diameter, speed and adding CMC to the solution are explained.

5.1 Polarization Curves

The linear polarization curve obtained for all the spheres in solution without CMC is shown in Figure 13. The polarization curves exhibit three regions. In the first region, the current increases with increasing potential. In this region the overall reaction is controlled by both mass transfer and electrochemical reaction. In the second region, the current becomes almost constant that manifests itself as a plateau in the polarization curve. The overall rate of reaction is determined by mass transfer only. The current corresponding to the plateau is called the limiting current and is recorded. In the third region, the current increases sharply associated with lots of gas bubbling on the electrode surface. This is due to the hydrolysis of water. The current in this region corresponds to the overall rate of reaction for hydrolysis of water.

In Figure 13, an increment is noticed in the current in the beginning. The experiment starts with 250 mV SCE and finished when the voltage reached to 650 mV. The plateau region was maintained for all the spheres at the same range between 450-550 mV. The current was constant over that voltage and this current is called the Limiting Diffusion Current (LDC).

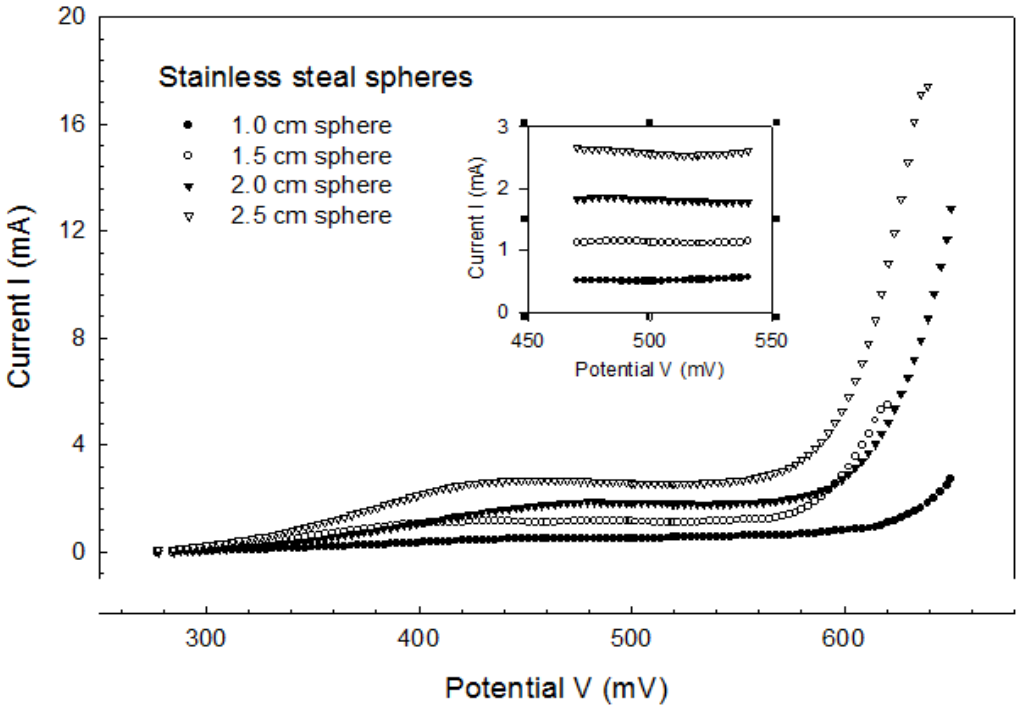

Figure 13 polarization curve for spheres in free solution

5.2 Chronoamperometric Curves

The Chronoamperometric Curves obtained for all the spheres in different solutions is shown in appendix A. The Chronoamperometric method is considered a good method to find the limiting diffusion current because of its short period. The maximum time observed in the experiments was around 1 minute. Once the voltage value is determined from the cycle voltammetry, this method will be used to find the rest of the value. In this work the chronoamperometric method was applied at 520 mV.

5.3 Newtonian Fluid

The mass transfer coefficients estimated by equation (2.4) are plotted against Sphere diameter for free solution in figure 14. The mass transfer coefficients decrease with increasing diameter of the sphere, conforming to the inferences of the boundary-layer theory that as the sphere diameter increases the boundary layer increase so lower mas transfer coefficient obtained.

The speed of the sphere was varied between 0 and 29.74 Rad/s to see the effect on the mass transfer coefficient. The results showed that for a given size of sphere, the mass transfer coefficient increase with increasing the rotational speed of the sphere. This is due to increasing the movement of ions when they are under motion, which will enhance ions to transfer between the working and counter electrodes. The mass transfer coefficients k_D is plotted against Sphere diameter at different speeds in Figure 15 and Figure 16. From

the plot, the maximum mass transfer coefficient was observed for 1.0 cm sphere at speed of 29.74 Rad/s.

Sherwood number was calculated for by knowing the mass transfer coefficient and the diffusivity of the ions in the solution. In fig.17 Sherwood number is plotted against Reynolds numbers for free fluid. The data exhibit power law relationship indicated by straight lines on logarithmic scale.

Noordsij et al [58] measured the mass transfer coefficient to a rotatoing sphere in pure solution using the same system and he developed a model for this case. Figure 18 shows the experimental data in agreement with the model developed by Noordsij with an average error of 4.7%. As result of this, the LDCT can be used further for the Non-Newtonian solution to evaluate the mass transfer coefficient.

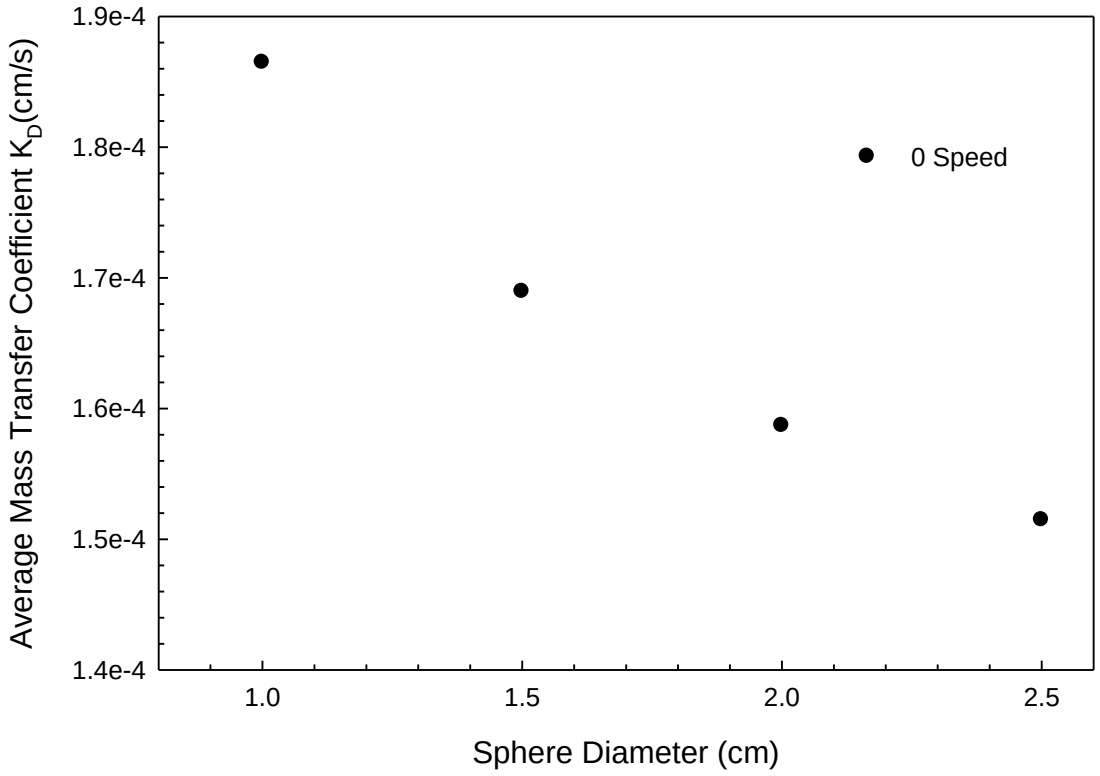

Figure 14 Mass transfer coefficient vs. sphere diameter in solution without CMC

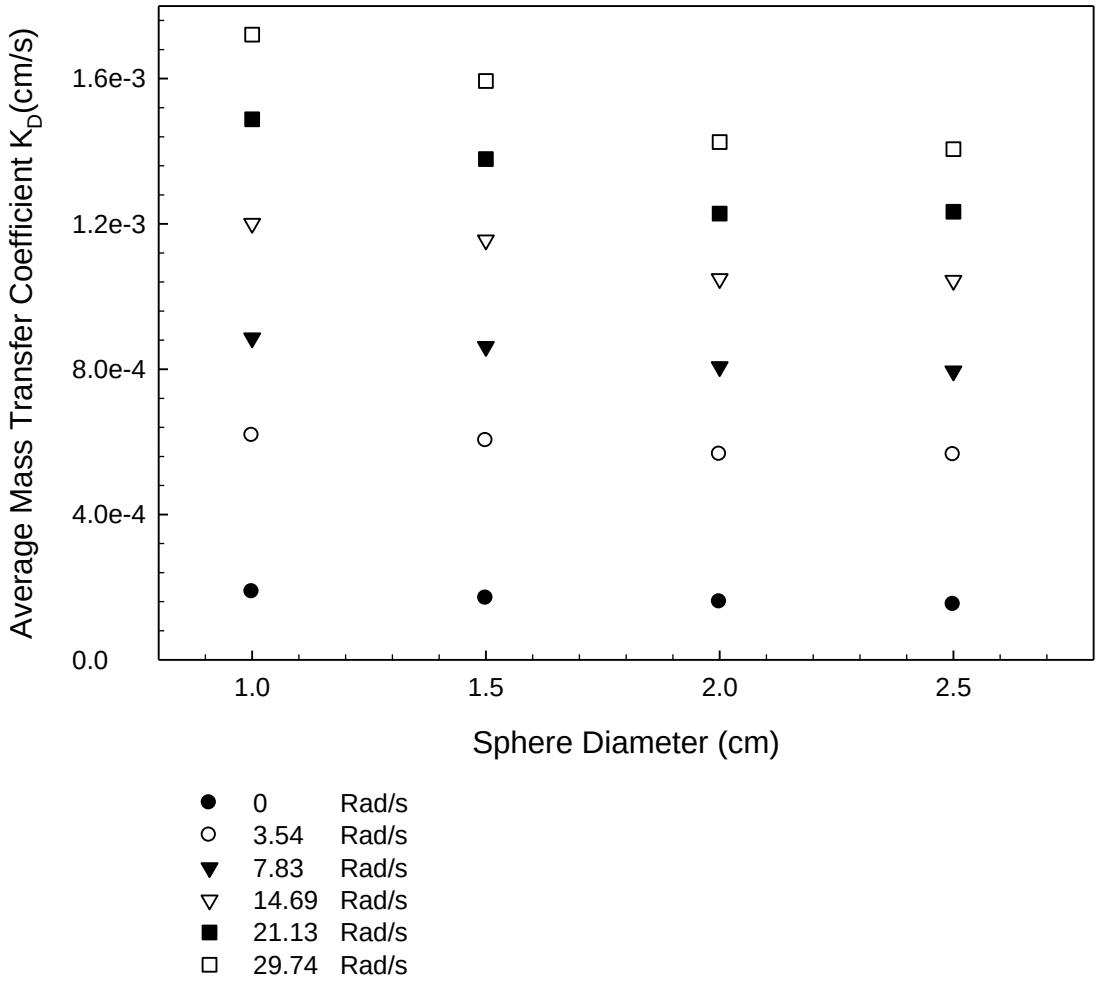

Figure 15 Mass transfer coefficient vs. sphere diameter at different speeds in solution without CMC

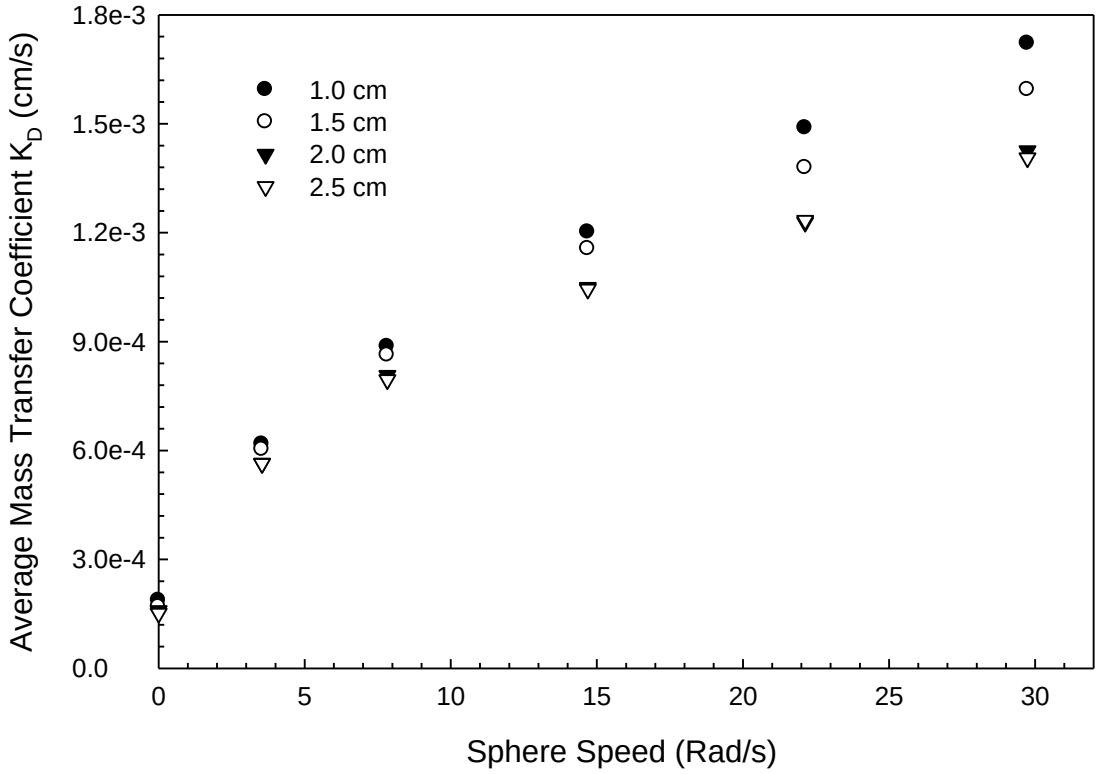

Figure 16 Mass transfer coefficient vs. sphere speed for different diameter in solution without CMC

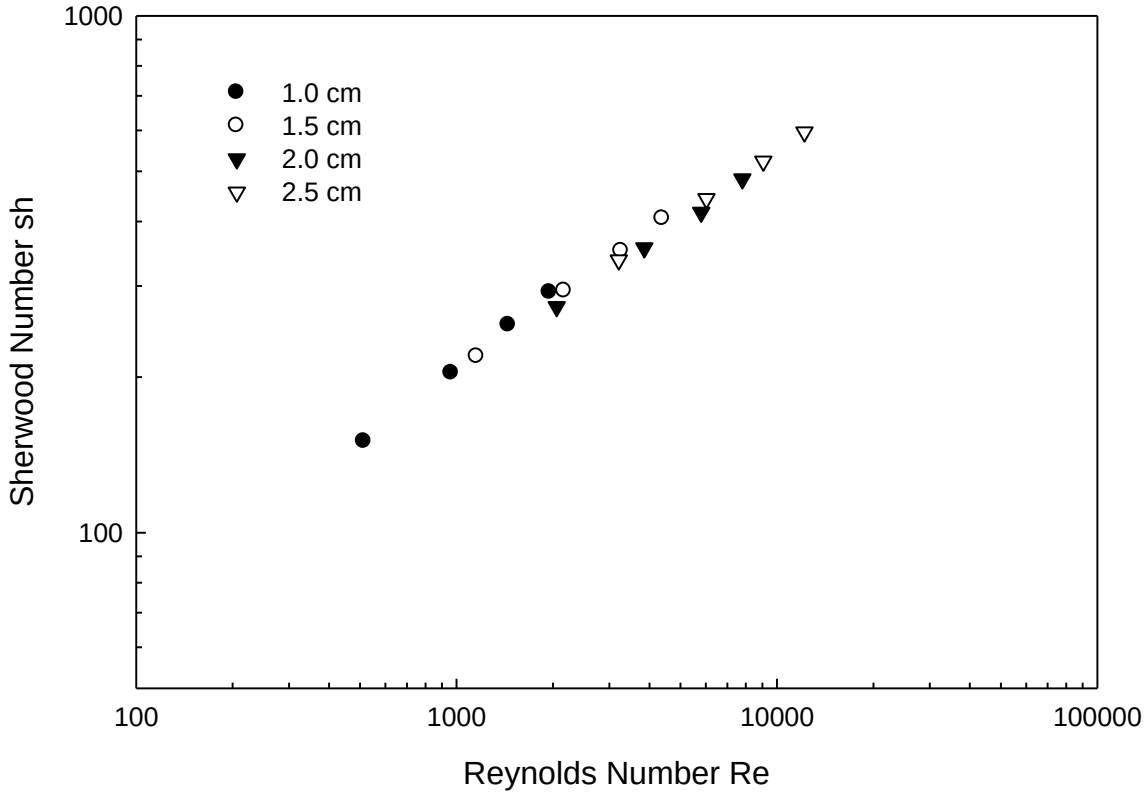

Figure 17 Sherwood number vs. Reynolds number for different sphere in solution without CMC

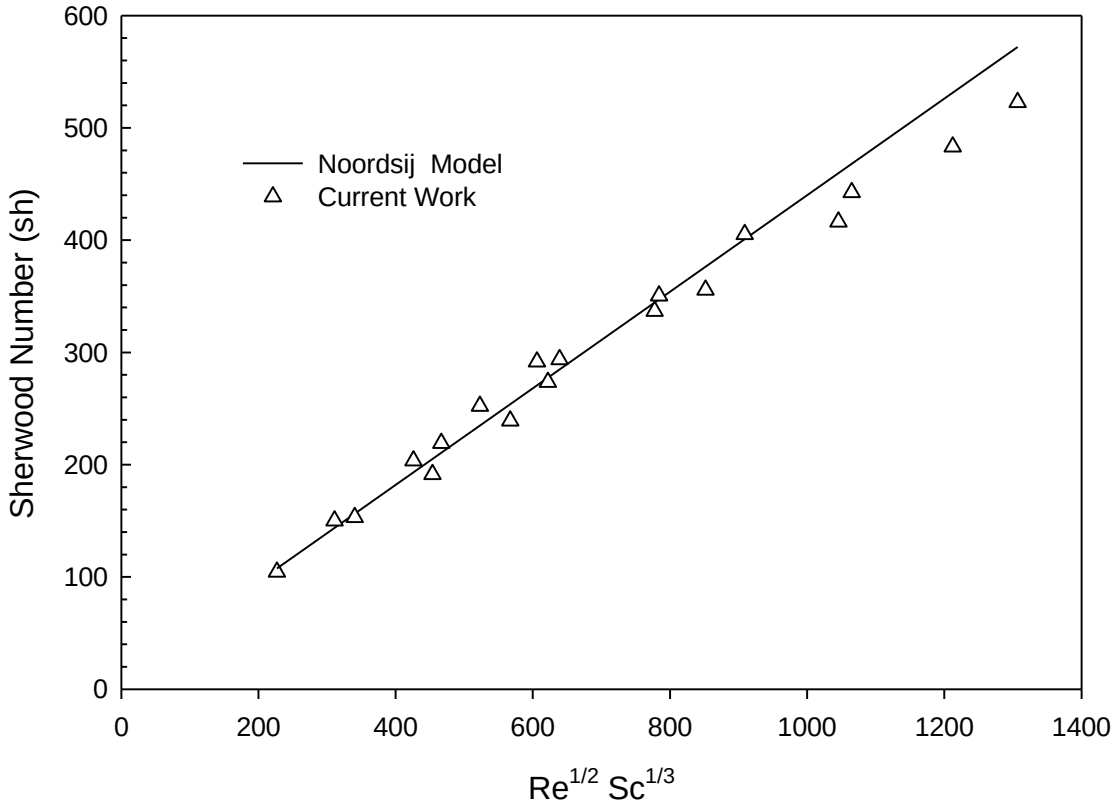

Figure 18 Comparison of Sherwood Number vs. $Re^{1/2}$ $Sc^{1/3}$ in free solution

5.4 Non-Newtonian Fluid

5.4.1 Polarization Curve

Polarization experiment was performed for 0.5 cm sphere in solution contains 5% of CMC. Figure 19 shows the polarization curve and the plateau exists over the same range as the Newtonian solution (0% of CMC). The chronoampermetric method was applied at 520mV to get the values of limiting diffusion current. Appendix A contains the chronoampermetric curves for all the experiments that were performed in the non-Newtonian part.

5.4.2 Effect of Spheres Diameter

The mass transfer coefficients estimated by Equation (2.4) are plotted against Sphere diameter for different solutions Figure 20. Similar to the case of natural convection in free solution, the mass transfer coefficients decrease with increasing diameter of the sphere, conforming to the boundary-layer theory. It was clear from the graph that a significant drop occurs in the mass transfer coefficient when the amount of CMC increased in the solution.

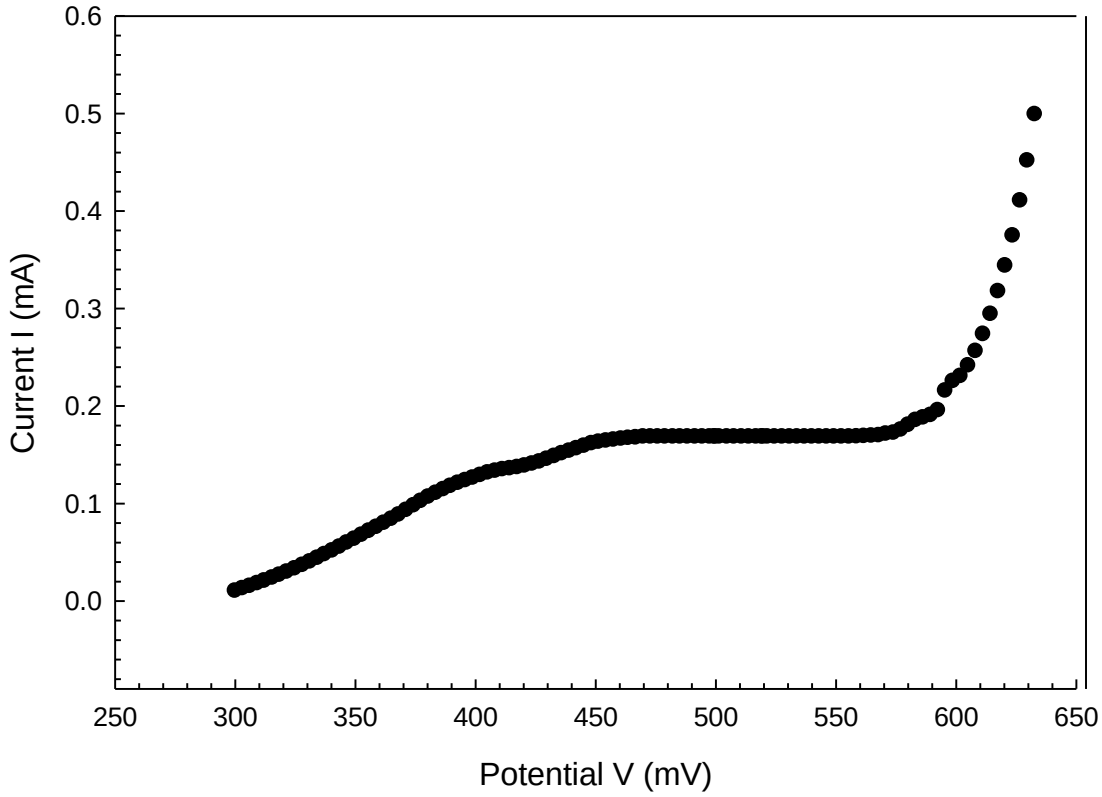

Figure 19 Polarization curve for 0.5cm sphere 5% CMC solution

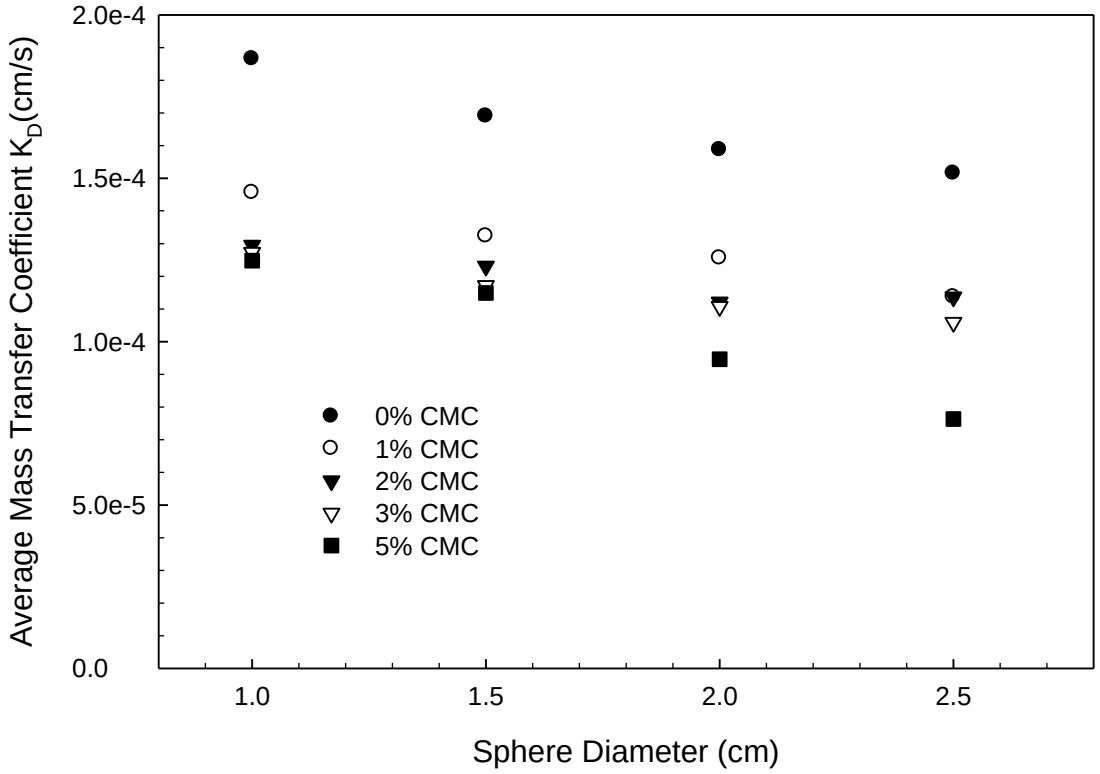

Figure 20 Mass transfer coefficient vs. sphere diameter in non-Newtonian solution

5.4.3 Effect of Rotational Speed

The effect of varying the speed on the mass transfer coefficient shows a strange relation at high percent of CMC as shown in Figure 21 through Figure 24. The same trend was observed for the mass transfer coefficient for the solution contains 1% of CMC with a little increment in the values of the mass transfer coefficient for the large diameter spheres at high speed. For 2% of CMC, the value of mass transfer coefficient of larger sphere exceeds the value of the lower diameter sphere at high speed. Further increment was noticed for 3% and 5% solutions. This behavior can be attributed to the nature of the solution. The non-Newtonian solutions, in this work are shear thing that is meaning the viscosity of the solution will decrease as the speed of the spheres increase. As result of this, the boundary layer thickness around the large sphere will decrease when it rotates. This explains why the mass transfer increases for large sphere in the non-Newtonian solution when the spheres rotate.

5.4.4 Effect of Adding CMC to the Solution

There is clear drop of the mass transfer coefficient after adding the CMC. The mass transfer coefficient is the highest in the case of free solution because of the low resistance to the rate of transfer. Figure 25 through 28 show the mass transfer coefficient as function of rotational speed for different spheres diameter at different percent of CMC. Further drop was noticed on the mass transfer coefficient when the amount of CMC was increase because of increasing the resistance of the ion to flow between the working and counter electrodes. The lowest values for the mass transfer coefficient are deducted when 5% of CMC was added to the solution.

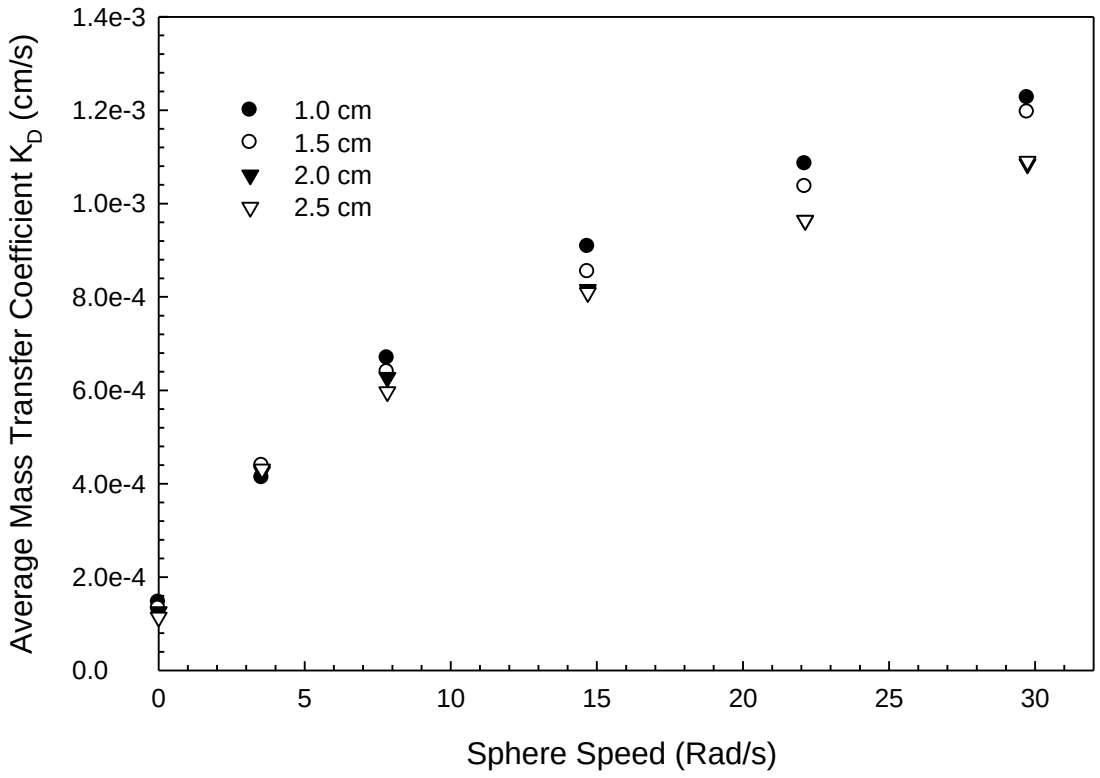

Figure 21 Mass transfer coefficient vs. sphere speed for different diameter in 1% CMC solution

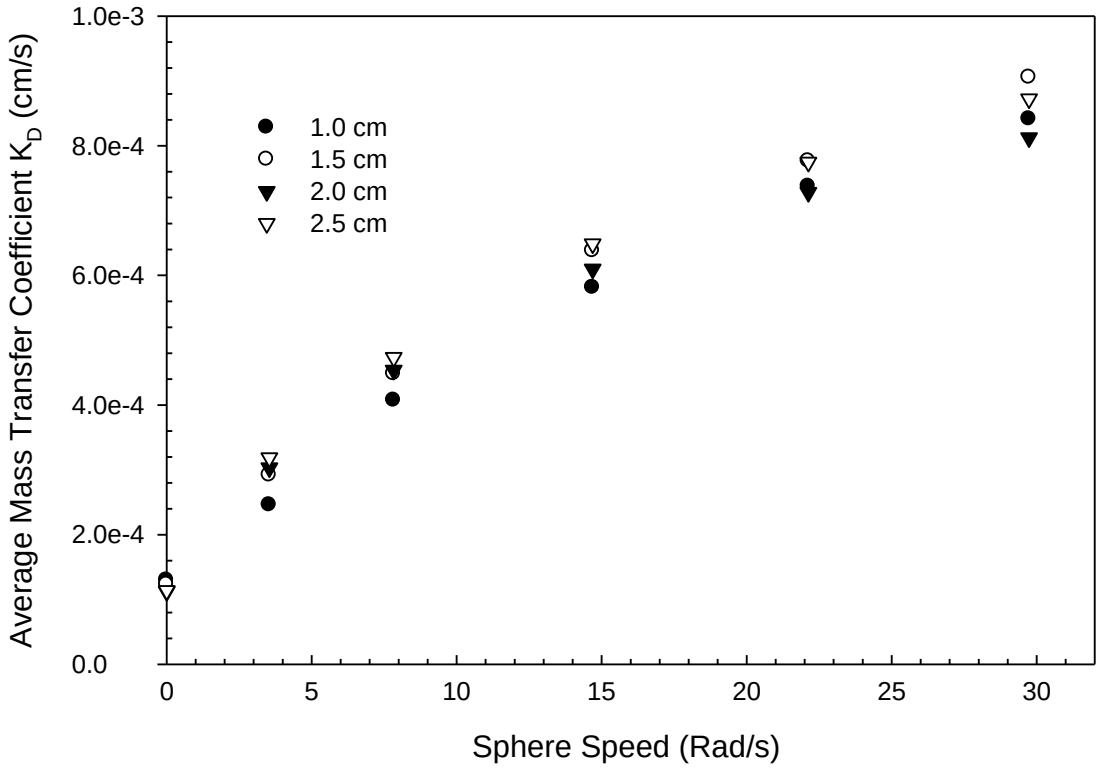

Figure 22 Mass transfer coefficient vs. sphere speed for different diameter in 2% CMC solution

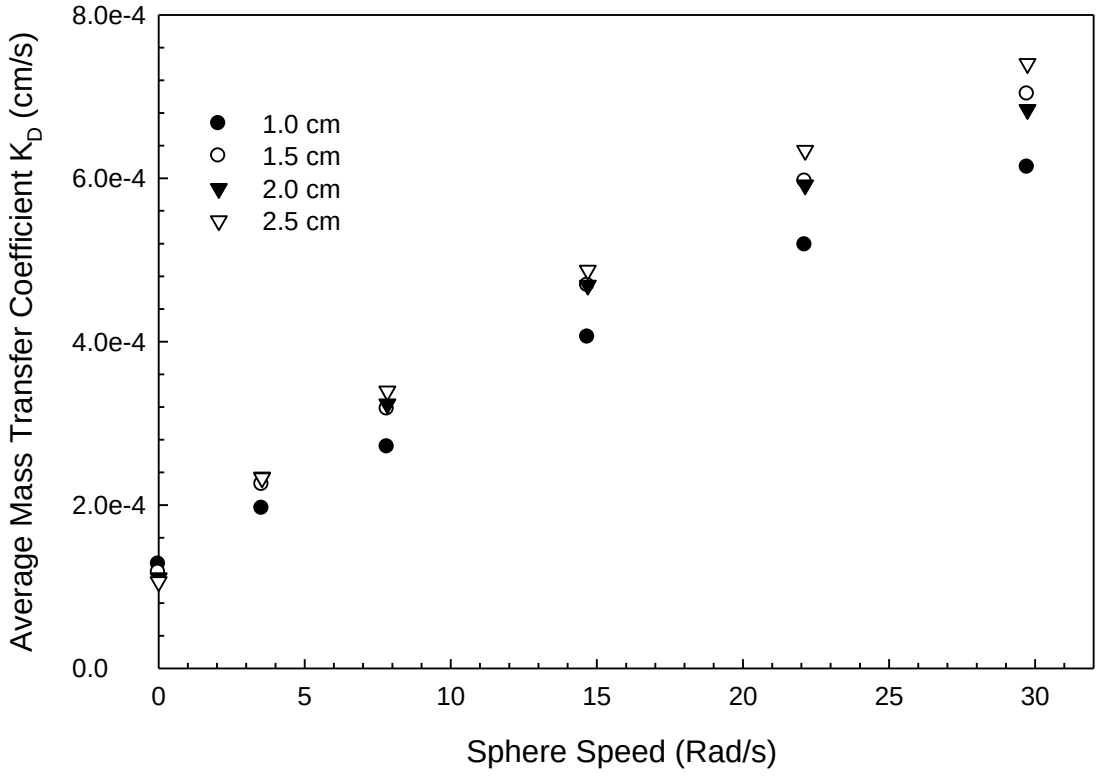

Figure 23 Mass transfer coefficient vs. sphere speed for different diameter in 3% CMC solution

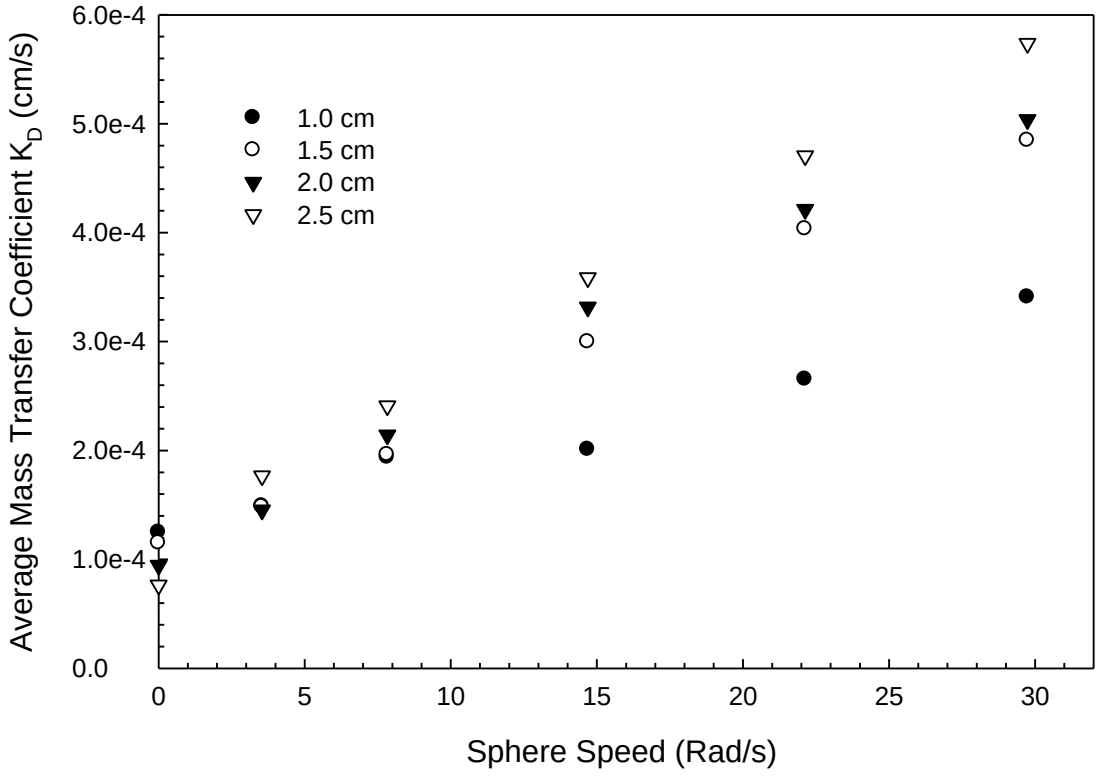

Figure 24 Mass transfer coefficient vs. sphere speed for different diameter in 5% CMC solution

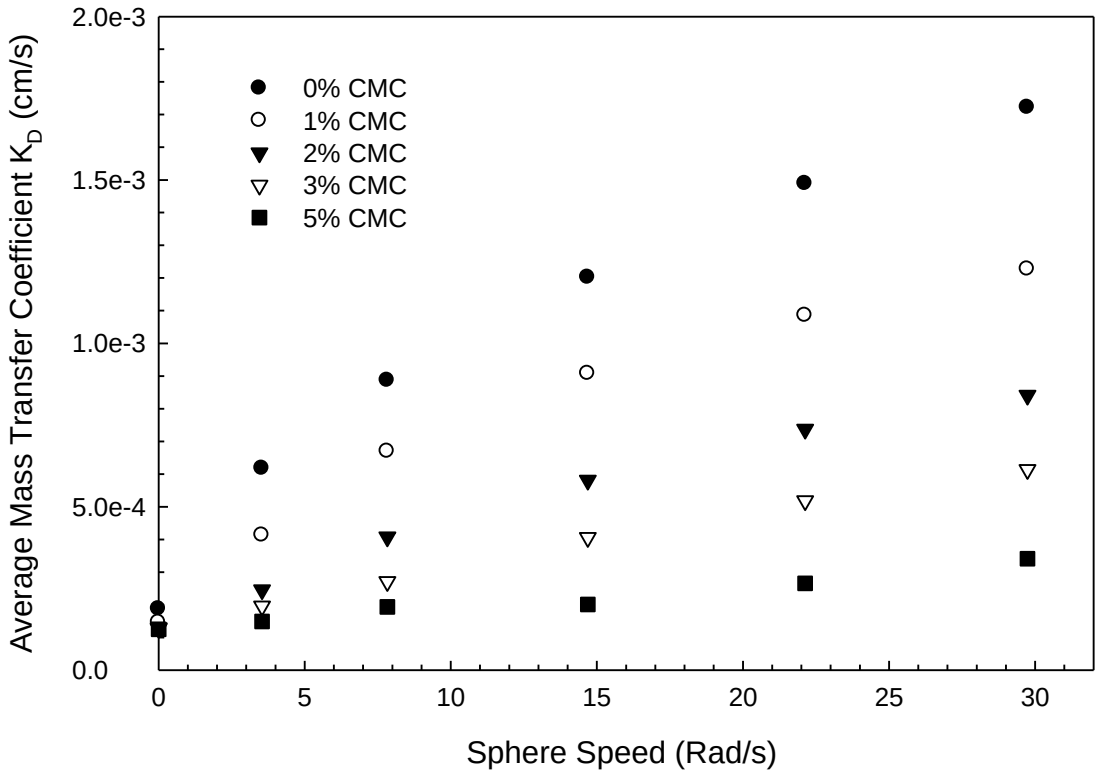

Figure 25 Mass transfer coefficient vs. sphere speed for 1.0 cm sphere in different solutions

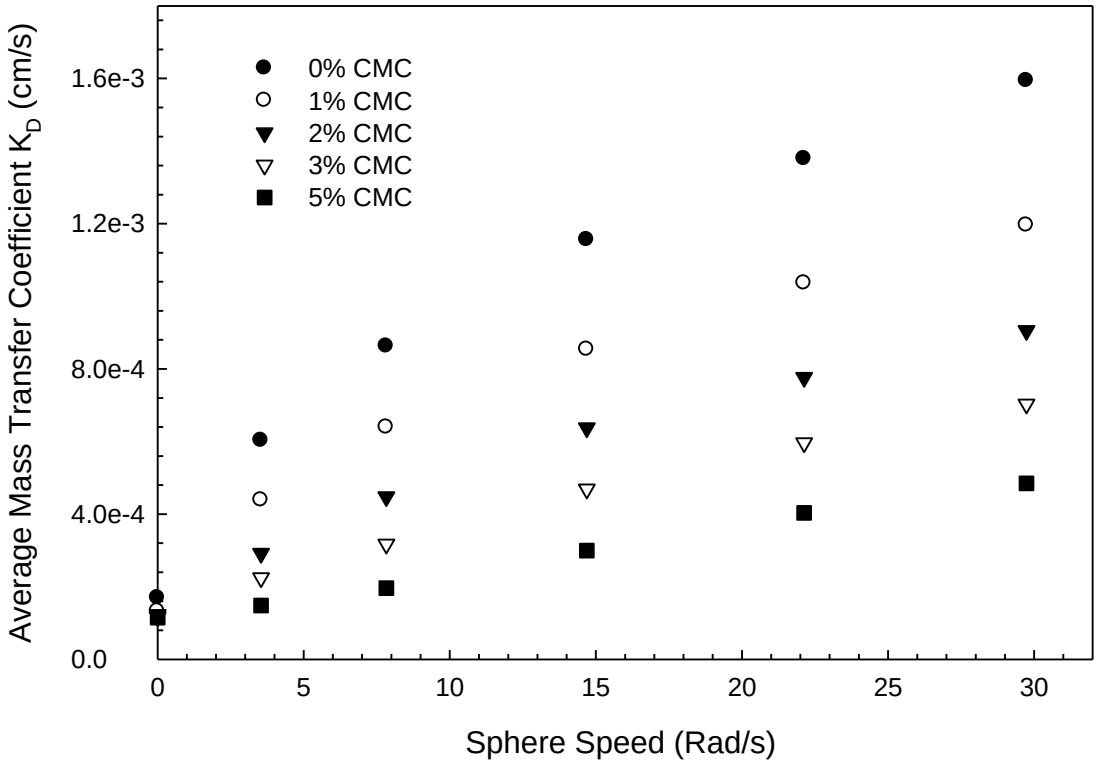

Figure 26 Mass transfer coefficient vs. sphere speed for 1.5 cm sphere in different solutions

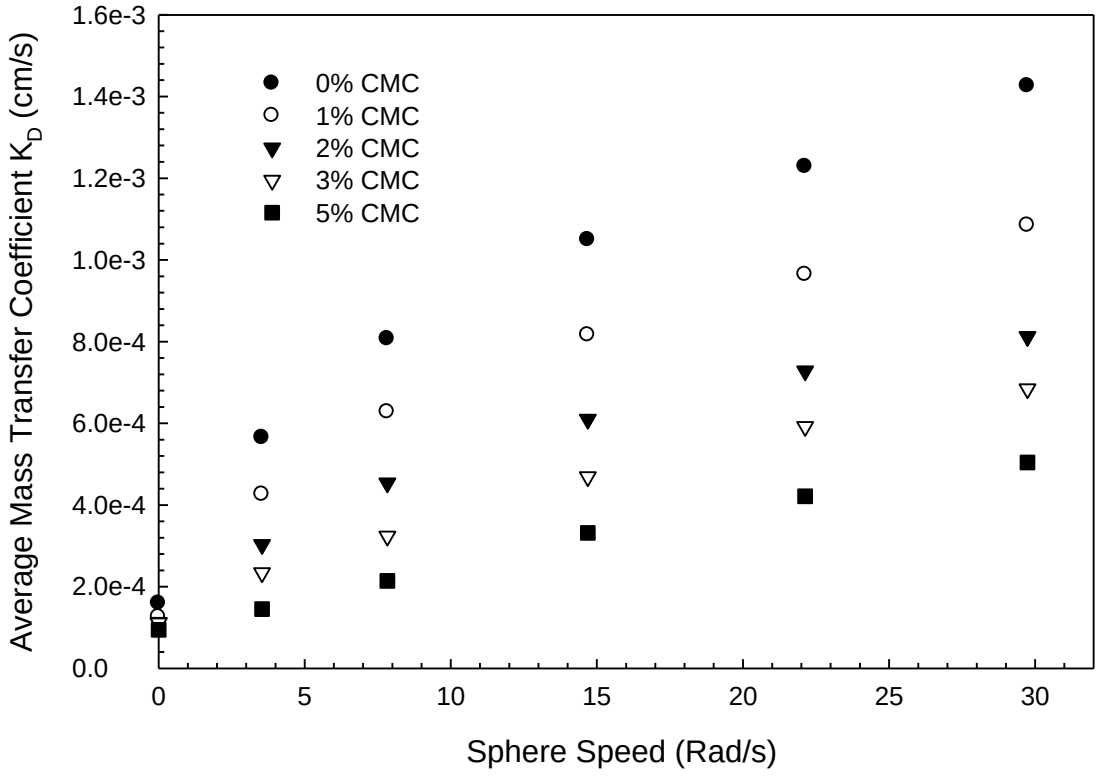

Figure 27 Mass transfer coefficient vs. sphere speed for 2.0 cm sphere in different solutions

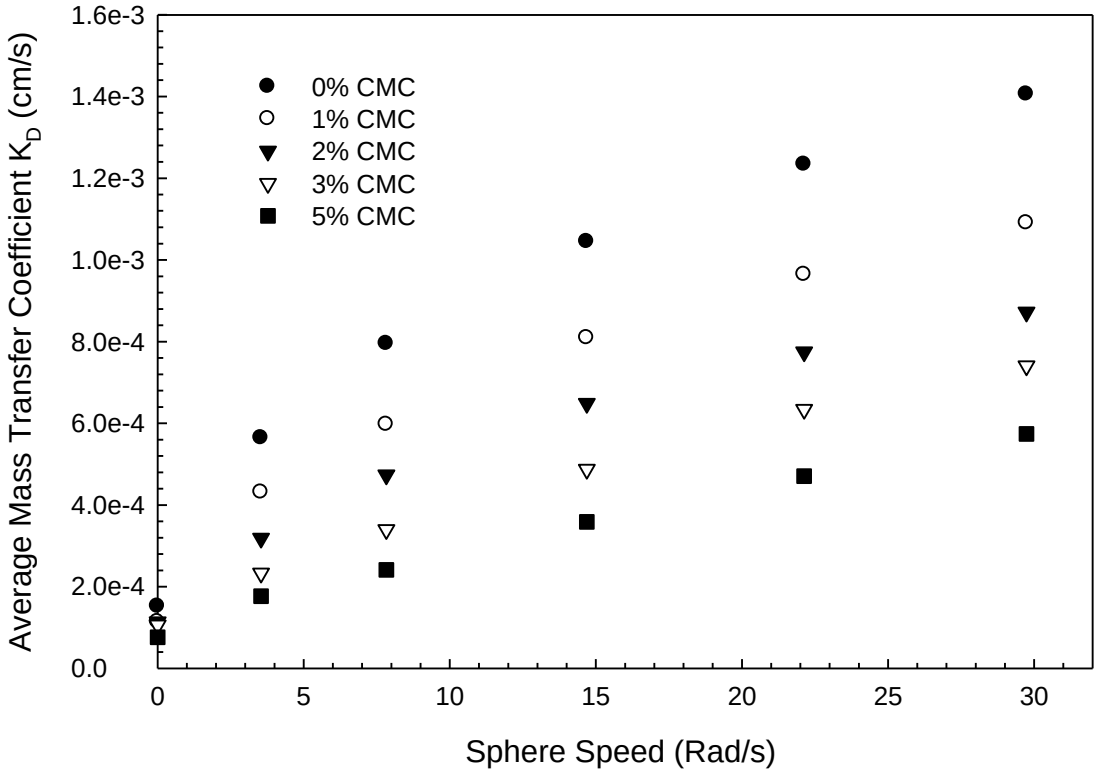

Figure 28 Mass transfer coefficient vs. sphere speed for 2.5 cm sphere in different solutions

5.4.5 Relation between Sherwood Numbers and (Re.Sc)

It was suggested by different researches that Sherwood number (Sh) is proportional to $Re^{1/2}$ $Sc^{1/3}$ in which, Reynolds (Re) and Schmit number (Sc). Therefore plots (Figure 29 through Figure 32) were made of Sh vs. $Re^{1/2}Sc^{1/3}$. A straight line relation was obtained which proof the validity of equation (5.1) for the non-Newtonian fluid. Table 12 shows the value of power index, consistency factor, A, m for all the solution.

$$Sh = A\left[\mathrm{Re}^{\frac{1}{2}}\, Sc^{\frac{1}{3}}\right]^{m} \tag{5.1}$$

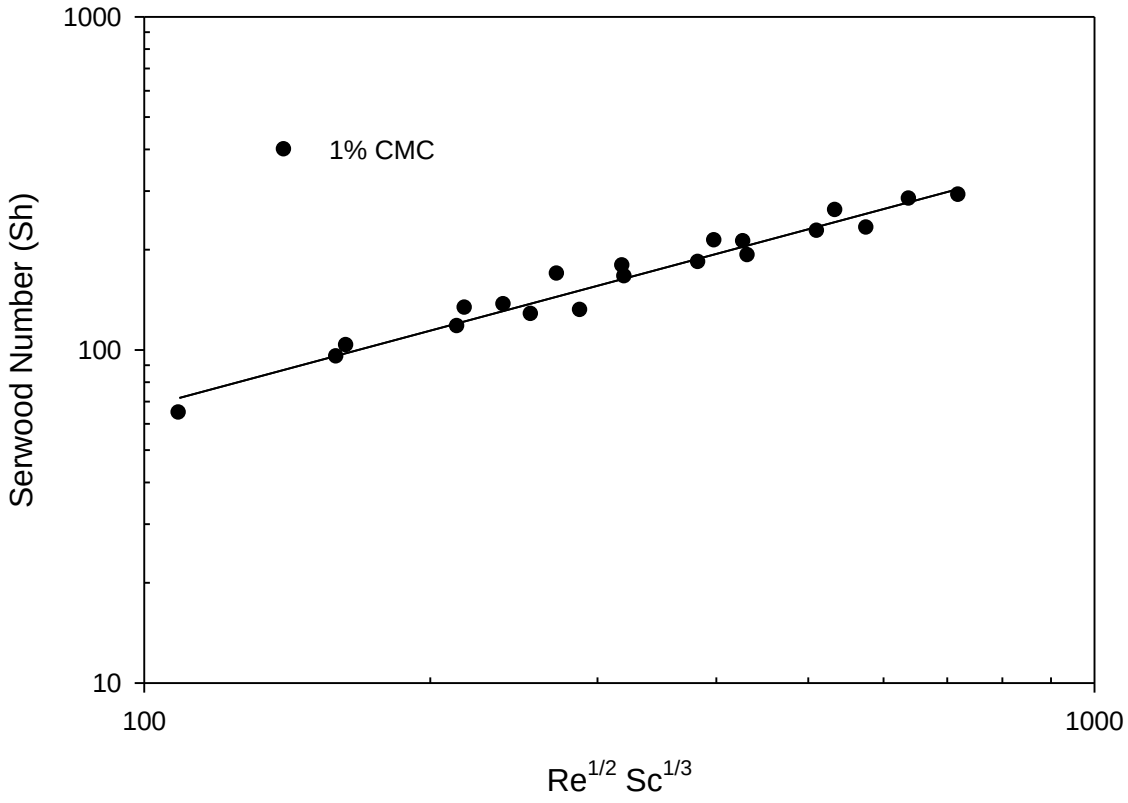

Figure 29 Sherwood number (Sh) vs. $Re^{1/2}Sc^{1/3}$ for 1% CMC solution

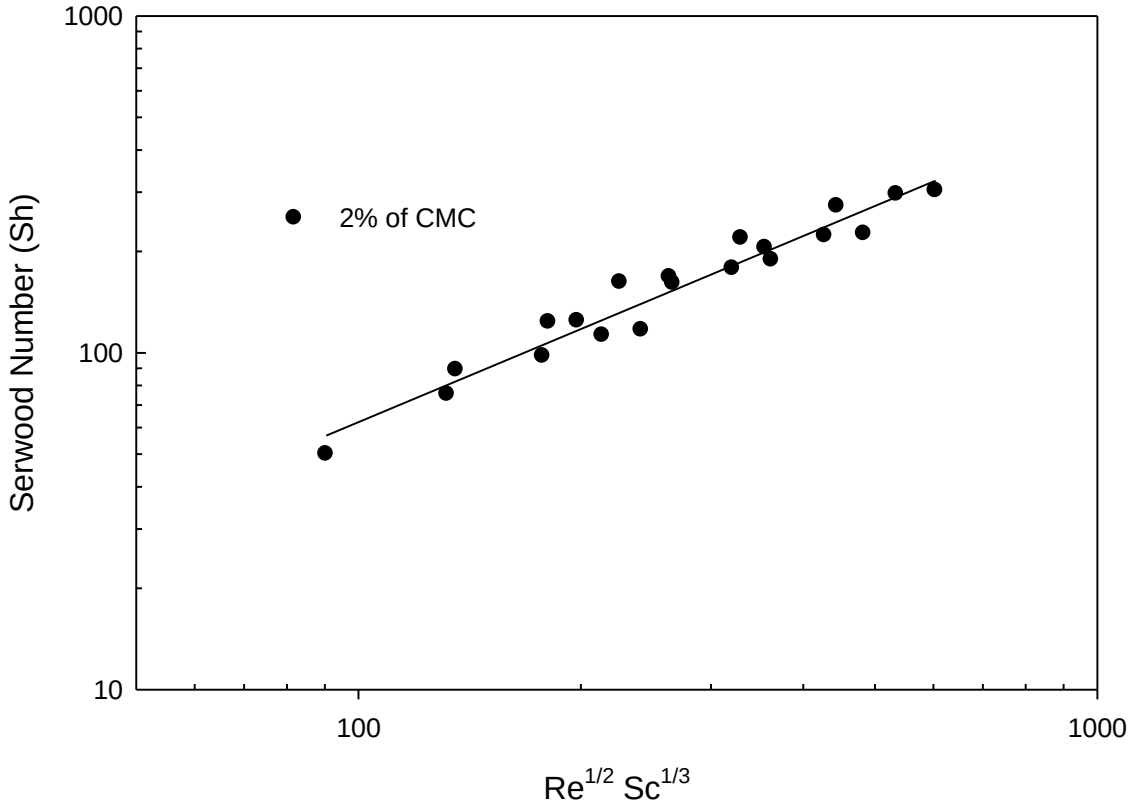

Figure 30 Sherwood number (Sh) vs. $Re^{1/2}Sc^{1/3}$ for 2% CMC solution

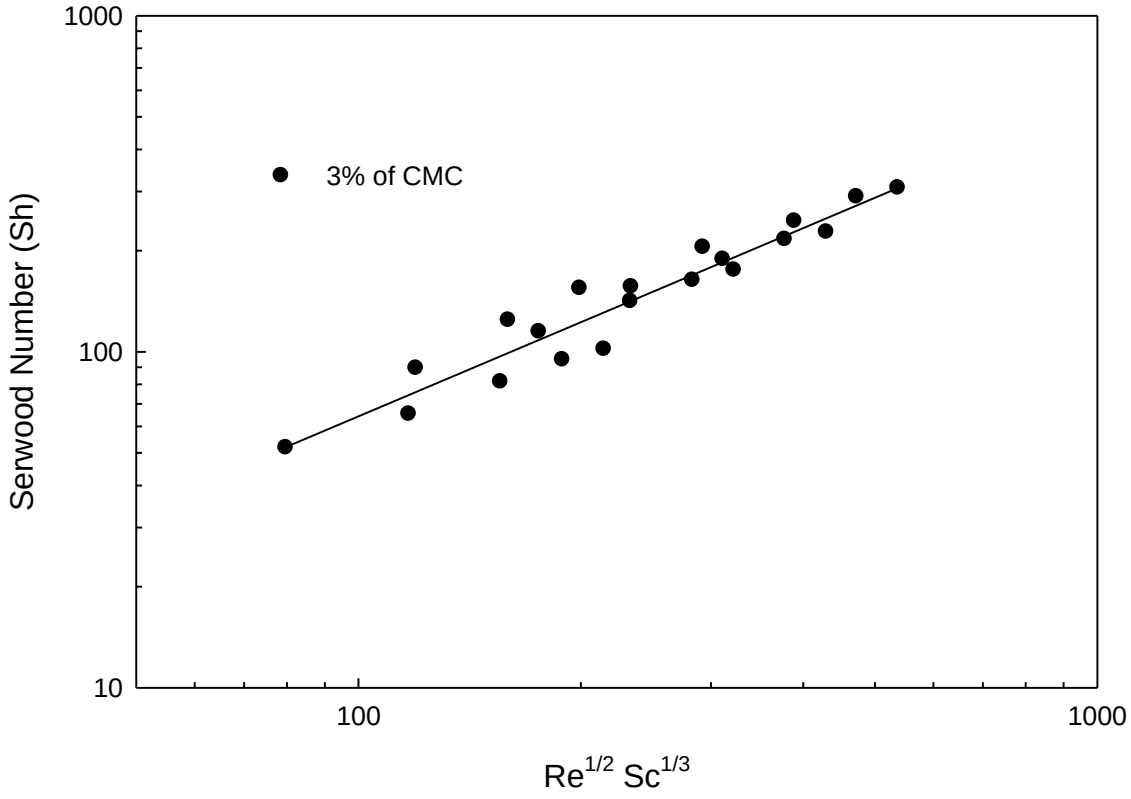

Figure 31 Sherwood number (Sh) vs. $Re^{1/2}Sc^{1/3}$ for 3% CMC solution

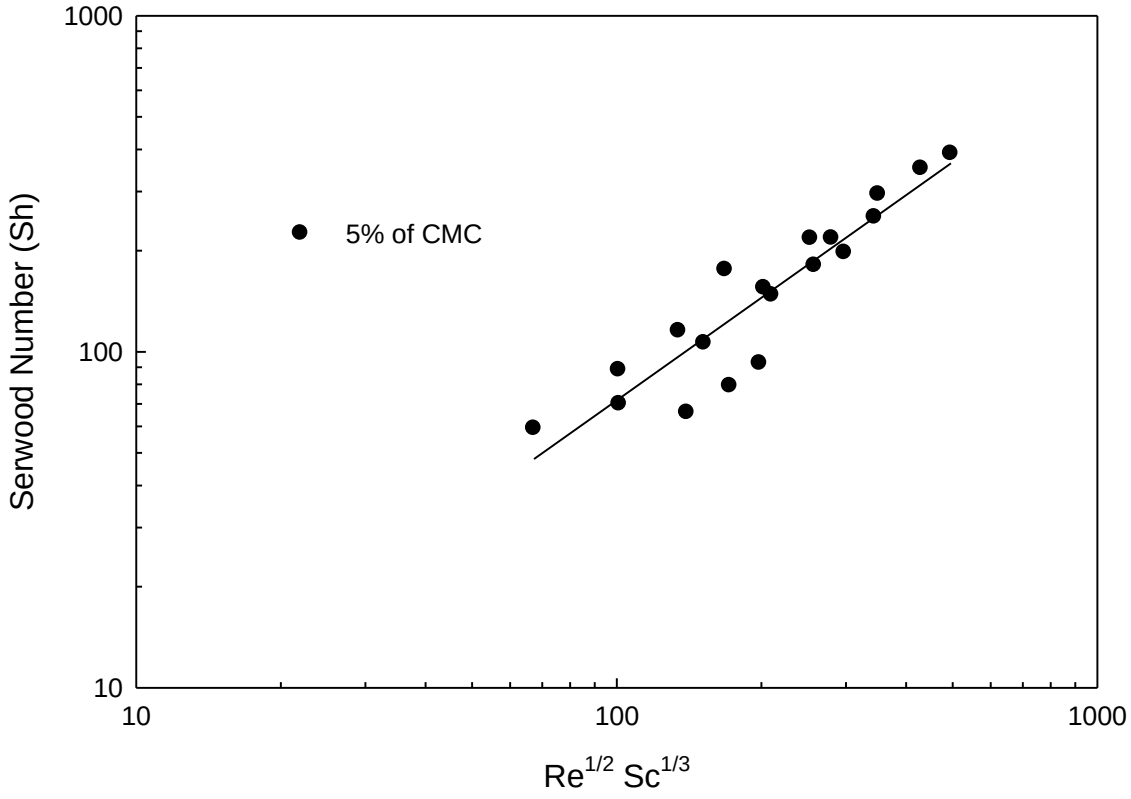

Figure 32 Sherwood number (Sh) vs. $Re^{1/2}Sc^{1/3}$ for 5% CMC solution

Table 12 the value of the slope, intercept, power index and consistency factor for all the solution

% of CMC	**n**	**K (Pa.s^n)**	**A**	**m**
1%	0.89	0.00743	1.975	0.766
2%	0.85	0.42	0.909	0.918
3%	0.777	1.59	0.886	0.930
5%	0.62	11.7	1.529	1.002

CHAPTER 6

CONCLUSION AND RECOMMENDATION

Mass transfer coefficients from spinning sphere in non-Newtonian solution were experimentally obtained. The limiting diffusion current technique (LDCT) has been used . Equimolar of ferri-ferrocyanide in addition to NaOH were used as an electrolyte in this work. spheres of stainless were fabricated to functioned as working electrode. The CMC (carboxymethyl cellulose) was added in different amount to make the Non-Newtonian solution.The effects of rotational velocity of the sphere, the size and the percent of CMC (carbxymethyl cellulose) in the solution were studied. Power index (n) and consistency factor (k) of the solution were obtained by measuring the stress of the solution at different shear rate using concentric cylinder viscometer. The diffusion coefficient of ferricyanide in sodium hydroxide was experimentally found from a method explained earlier by Noordsij. Average Sherwood numbers were calculated and data were compared with existing mathematical models. Good agreement between the data obtained in this study and the one proposed by Noordsij was noticed for the Newtonian solution. The results of the experiments with different loading of CMC showed that Sherwood number (Sh) is proportional to $Re^{1/2}$ $Sc^{1/3}$, in which Re and Sc are Reynolds and Schmidt numbers, respectively. This work was done using sphere geometry which can simulate the drilling bit in the petroleum industry. I would recommend if different geometries such as cylinder is used to study the mass transfer coefficient.

References

[1] J.R. Selman, C.W. Tobias, Mass-transfer measurements by the limiting-current technique, Adv. Chem. Eng. 10 (1988) 211–318.

[2] T. Nishimura, N. Kojima, Mass transfer enhancement in a symmetric sinusoidal wavy-walled channel for pulsate flow, Int. J. Heat Mass Transfer 38 (1995) 1719–1731.

[3] L. Broniarz-Press, J. Bednarz, J. Rozanski, Mass transfer enhancement in Newtonian and non-Newtonian liquids flowing in channels of the sinusoidal shape, Int. J. Appl. Mech. Eng. 10 (2005) 93–98.

[4] M. Gradeck, M. Lebouche_, Wall shear measurements inside corrugated channels using the electrochemical technique, Exp. Fluids 24 (1998) 17–26.

[5] L. Broniarz-Press, J. Rozanski, J. Bednarz, Intensity of mass transfer in Newtonian and non-Newtonian liquids flowing in sinusoidal channels, in: Proceedings of the Third International Conference on Transport Phenomena in Multiphase Systems ‘‘HEAT 2005”, Gdansk, 26–30 June 2005, IFFM Publishers, Gdansk, 2005, pp. 229–234.

[6] G. Schu¨ tz, Natural convection mass transfer measurements on spheres and horizontal cylinders by an electrochemical method, Int. J. Heat Mass Transfer 6 (1963) 873–879.

[7] P.N. Pintauro, An electrochemical method for determining natural convection mass transfer boundary-layer thickness, Int. J. Heat Mass Transfer 29 (1986) 741–751.

[8] H.D. Doan, M.E. Fayed, O. Trass, Measurement of local and overall mass-transfer coefficients to a sphere in a quiescent liquid using a limiting current technique, Chem. Eng. J. 81 (2001) 53–61.

[9] J. Tihon, V. Tovchigrechkov, V. Sobolik, O. Wein, Electrodiffusion detection of the near-wall flow reversal in liquid films at the regime of solitary waves, J. Appl. Electrochem. 33 (2003) 577–587.

[10] V. Sobolik, O. Wein, J. Cermak, Simultaneous measurement of film thickness and wall shear stress in wavy flow of non-Newtonian liquids, Collect. Czechoslov. Chem. Commun. 52 (1987) 913– 928.

[11] F.P. Berger, K-F. Hau, Mass transfer in turbulent pipe flow measured by the electrochemical method, Int. J. Heat Mass Transfer 20 (1977) 1185–1194.

[12] W. Zhao, O. Trass, Electrochemical mass transfer measurements in rough surface pipe flow: geometrically similar V-shaped grooves, Int. J. Heat Mass Transfer 40 (1997) 2785 2797.

[13] J. Tihon, C. Deslouis, B. Tribollet, Structure of the near-wall turbulence in a drag-reducting flow, in: Proceedings of the Fifth European Rheology Conference, Portoroz, 1998, pp. 163–164.

[14] N. Mahinpey, M. Ojha, O. Trass, Transient mass and heat transfer in a smooth pipe, Int. J. Heat Mass Transfer 44 (2001) 3919– 3930.

[15] G. Bartelmus, Experimental determination of the mass transfer coefficients on the solid phase-liquid interface in packed columns. I. The electrochemical method fundamentals of the measure method of the transfer coefficients kLS, Chem. Process Eng. (Poland) 7 (1986) 527–543.

[16] X.-S. Zhang, G.-B. Wu, P. Ding, X.-G. Zhou, W.-K. Yuan, Studies on paired packed-bed electrode reactor: modelling and experiments, Chem. Eng. Sci. 54 (1999) 2969–2977.

[17] T. Ravi, B.S. Rao, K.P. Krishna, P. Venkateswarlu, Ionic mass transfer studies in fluidised beds with coaxially placed discs on a rod as internal, Chem. Eng. Process. 35 (1996) 187–193.

[18] K. Bouzek, J. Palmer, I. Rousar, A.A. Wragg, Mass transfer to wall electrodes in a fluidised bed of inert particles, Electrochim. Acta 44 (1996) 583–599.

[19] D.W. Hall, K. Scott, R.J.J. Jachuck, Determination of mass transfer coefficient of a cross-corrugated membrane reactor by the limitingcurrent technique, Int. J. Heat Mass Transfer 44 (2001) 2201–2207.

[20] Merk, H.J., Prins, J.A., 1953–1954. Thermal convection in laminar boundary layers I, II. Applied Scientific Research A4, 11–24 195–206.

[21] Chiang, T.,Ossin,A.,Tien,C.L.,1964.Laminarfreeconvectionfromasphere. Journal ofHeatTransfer86,537–542.

[22] Stewart, W.E., 1971. Asymptotic calculation of free convection in laminar three-dimensional systems. International Journal of Heat and Mass Transfer 14, 1013–1031.

[23] Potter, J.M., Riley, N., 1980. Free convection from a heated sphere at large Grashof number. Journal of Fluid Mechanics 100, 769–783.

[24] Jafarpur, K., Yovanovich, M.M., 1992. Laminar free convective heat transfer from isothermal spheres: a new analytical method. International Journal of Heat and Mass Transfer 35, 2195–2201.

[25] Fendell, F.E.,1968.Laminarnaturalconvectionaboutanisothermallyheated sphere atsmallGrashofnumber.JournalofFluidMechanics34,163–176.

[26] Singh, S.N., Hasan, M.M., 1983. Free convection about a sphere at small Grashof number. International Journal of Heat and Mass Transfer 25, 781–783.

[27] Geoola, F.,Cornish,A.R.H.,1981.Numericalsolutionofsteady-statefreeconvective heat transferfromasolidsphere.InternationalJournalofHeatandMass Transfer 24,1369–1379.

[28] Geoola,F.,Cornish,A.R.H.,1982.Numericalsolutionoffreeconvectiveheattransfer fromasphere.InternationalJournalofHeatandMassTransfer25,1677–1687.

[29] Farouk, B.,1982.Naturalconvectionheattransferfromanisothermalsphere.In: Proceedings ofthe16thSoutheasternThermalSciencesConference,Miami,FL, pp. 347–364.

[30] Fujii, T.,Honda,T.,Fujii,M.,1984.Anumericalanalysisoflaminarfreeconvection around anisothermalsphere:finitedifferencesolutionofthefullNavier– Stokes and energy equationsbetweenconcentricspheres.NumericalHeat Transfer 7,103–111.

[31] Riley, N., 1986. The heat transfer from a sphere in free convective flows. Computers and Fluids 14, 225–237.

[32] Takamatsu, H., Fujii, M., Fujii, T., 1988. A numerical analysis of free convection around an isothermal sphere (effects of space and Prandtl number). JSME International Journal Series II 31, 66–72.

[33] Dudek, D.R.,Fletcher,T.H.,Longwell,J.P.,Sarofim,A.F.,1988.Naturalconvection induced dragforcesonspheresatlowGrashofnumbers:comparisonoftheory with experiment.InternationalJournalofHeatandMassTransfer31,863–873.

[34] Johnson, A.T., Kirk, G.D., Moon, S.H., Shih, T.M., 1988. Numerical and experimental analysis of mixed forced and natural convection about a sphere. Transactions of ASAE 31, 293–304.

[35] Jia, H., Gogos, G., 1996a. Laminar natural convection heat transfer from isothermal sphere. International Journal of Heat and Mass Transfer 39, 1603–1615.

[36] Jia, H., Gogos, G., 1996b. Transient laminar natural convection heat transfer from isothermal sphere. Numerical Heat Transfer A 29, 83–101.

[37] Yang, S., Raghavan, V., Gogos, G., 2007. Numerical study of transient laminar natural convection over an isothermal sphere. International Journal of Heat and Fluid Flow 28, 821–837.

[38] Amato, W.S., Tien, C., 1972. Free convection heat transfer from isothermal spheres in water. International Journal of Heat and Mass Transfer 15, 327–339.

[39] Acrivos, A., 1960. A theoretical analysis of laminar natural convection heat transfer to non-Newtonian fluids. AIChE Journal 6, 584–590.

[40] Liew, K.S., Adelman, M., 1975. Laminar natural heat transfer from an isothermal sphere to non-Newtonian fluids. The Canadian Journal of Chemical Engineering 53, 494–499.

[41] Amato, W.S., Tien, C., 1976. Free convection heat transfer from isothermal spheres in polymer solutions. International Journal of Heat and Mass Transfer 19, 1257–1266.

[42] Churchill, S.W.,1983.Comprehensivetheoreticalbased,correlatingequationsfor free convectionfromisothermalspheres.ChemicalEngineeringCommunica- tions 24,339–352.

[43] Lee, T.-L., Donatelli, A.A., 1989. Mass transfer by natural convection from a solid sphere to power-law fluids. Industrial and Engineering Chemistry Research 28, 105–107.

[44] Churchill, S.W.,Churchill,R.U.,1975.Acomprehensivecorrelatingequationfor heat andcomponenttransferbyfreeconvection.AIChEJournal21,604–606.

[45] A. Prhashanna, R.P. Chhabra, 2010. Free convection in power-law fluids from a heated sphere. Chemical Engineering Science 65, 6190–6205.

[46] Han-Taw Chen and Cha' o-Kuang Chen, 1988. Natural Convection of a non-newtonian fluid about a horizontal cylinder and a sphere in a porous medium. Int. Comm. Heat Mass Transfer 15, 605–614.

[47] S. G. Stokes, On the theories of the internal friction of fluid in motion, Camb. Trans. 8,287 (1845).

[48] B. Farouk. Mixed convective Row around a slowly rotating isothermal sphere. Trs. ASME: J. Heat Transfere 107,431438 (1985).

[49] F. S. Lien, C. K. Chen and J. W. Cleaver. Mixed and free convection over a rotating sphere with blowing and suction. Trans. ASME: J. Heat/Transfer 108, 398404 (1986).

[50] G. L. Palec and M. Daguenet, Laminar three-dimensional mixed convection about a rotating sphere in stream, Int. J. Heat/ Mass transfer 30, 1511-1523 (1987).

[51] T. S. Chcn and A. Mucoglu, Analysis of mixed forced and free convection about a sphere, Int. J. Heat/ Mass transfer 20, 867-875 (1977).

[52] P. Hatzikonstantinou. Unsteady mixed convection about a porous rotating sphere, Int. J. Heat/ Mass transfer. 33, I 9-27 (1990).

[53] T. Yuge, Experiments on heat transfer from sphere including combined. natured and forced convection, ASME Trans. Ser. C 82.2 I4220 (1960).

[54] L. A. Dorfman and A. Z. Serazetdinov, Laminar flow and heat transfer near rotating axisymmetric surface, Int. J. Heat Mass transfer 8, 3 17-327 (1965). (1984).

[55] F. Kreith, L. G. Roberts, J. A. Sullivan and S. N. Sinha, Convection heat transfer and flow phenomena of rotating sphere, Int. J. Heat Mass Transfer 6, 88 l-895 (1963).

[56] W. H. Banks, The thermal laminar boundary layer on rotating sphere, J. Appl. Math. Phys. 16, 780-788 (1965).

[57] S. M. Tieng, C. Yan, Experimental investigation on convective heat transfer of heated spinning sphere, Int. J. Heat Mass Transfer 36, 599-610 (1993).

[58] P. Noorgsij, W. Rotte, Mass Transfer coefficients to a rotating and to a vibrating sphere, Chem Engng Sci. 22, 1475-1481 (1967).

Appendix-A

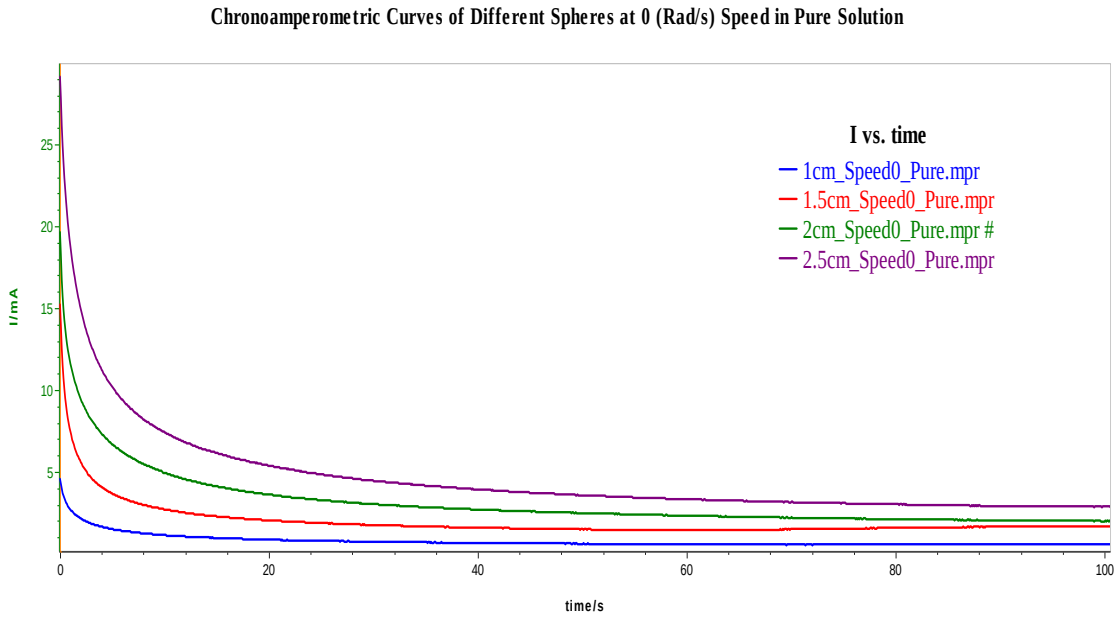

Figure A1: Chronaperometric curves of different spheres at 0 (Rad/s) speed in pure solution

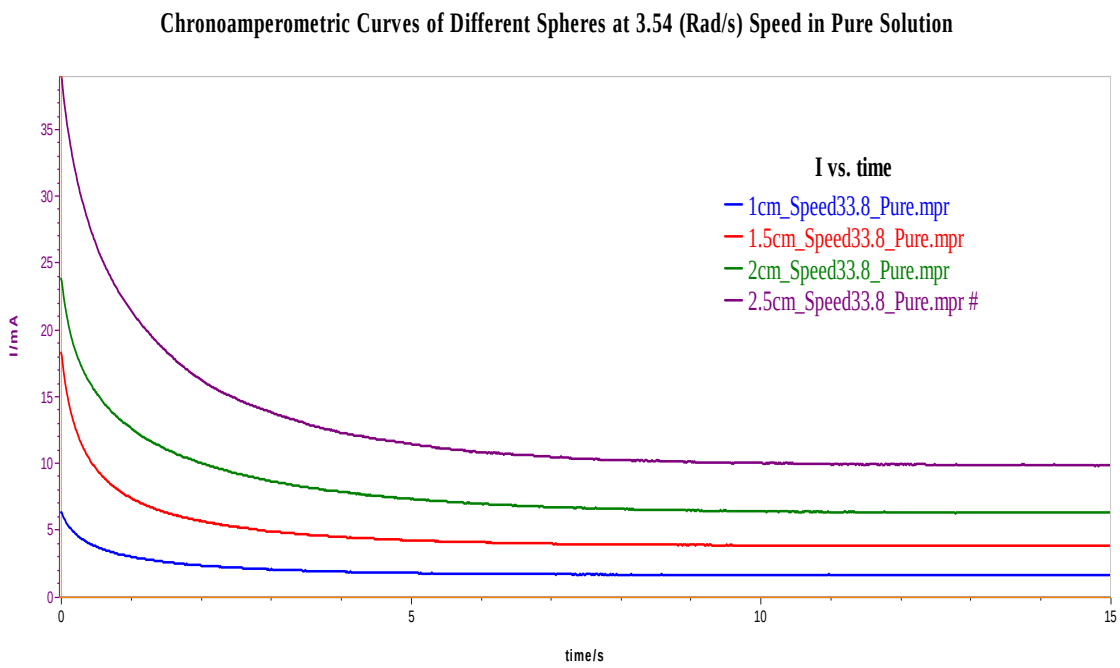

Figure A2: Chronaperometric curves of different spheres at 3.54 (Rad/s) speed in pure solution

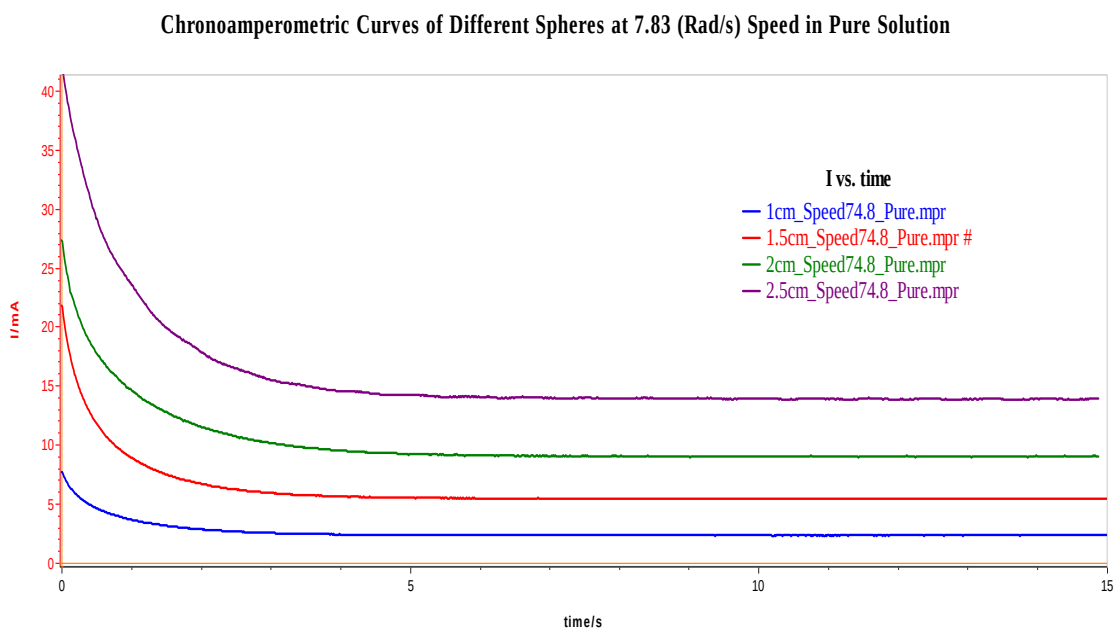

Figure A3: Chronaperometric curves of different spheres at 7.83 (Rad/s) speed in pure solution

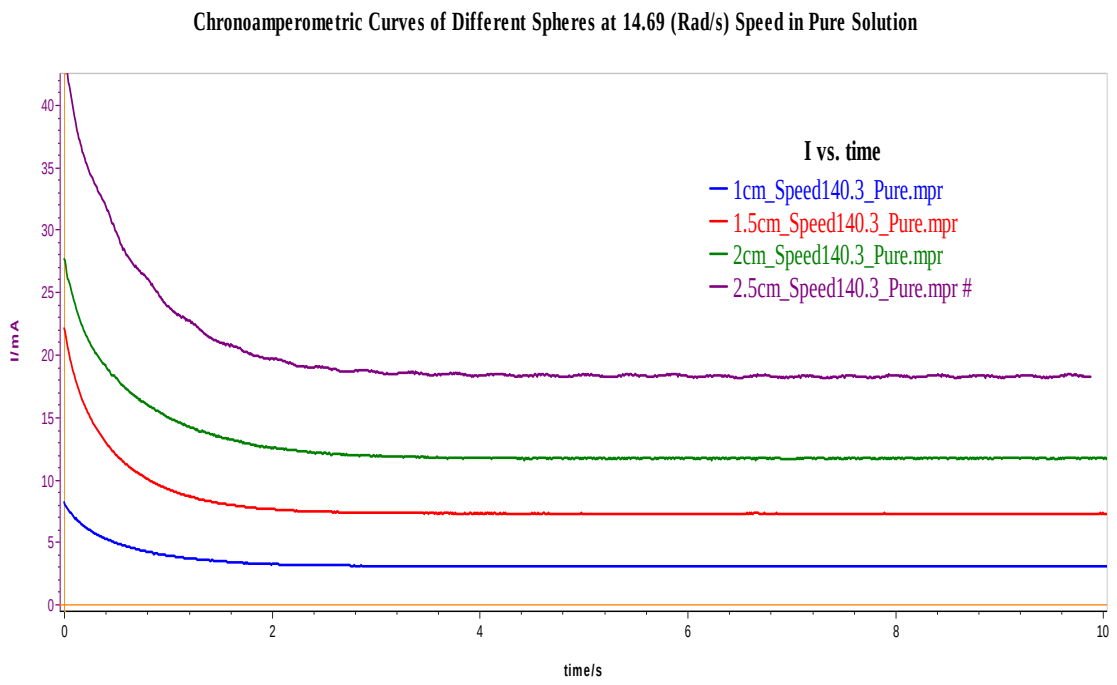

Figure A4: Chronaperometric curves of different spheres at 14.69 (Rad/s) speed in pure solution

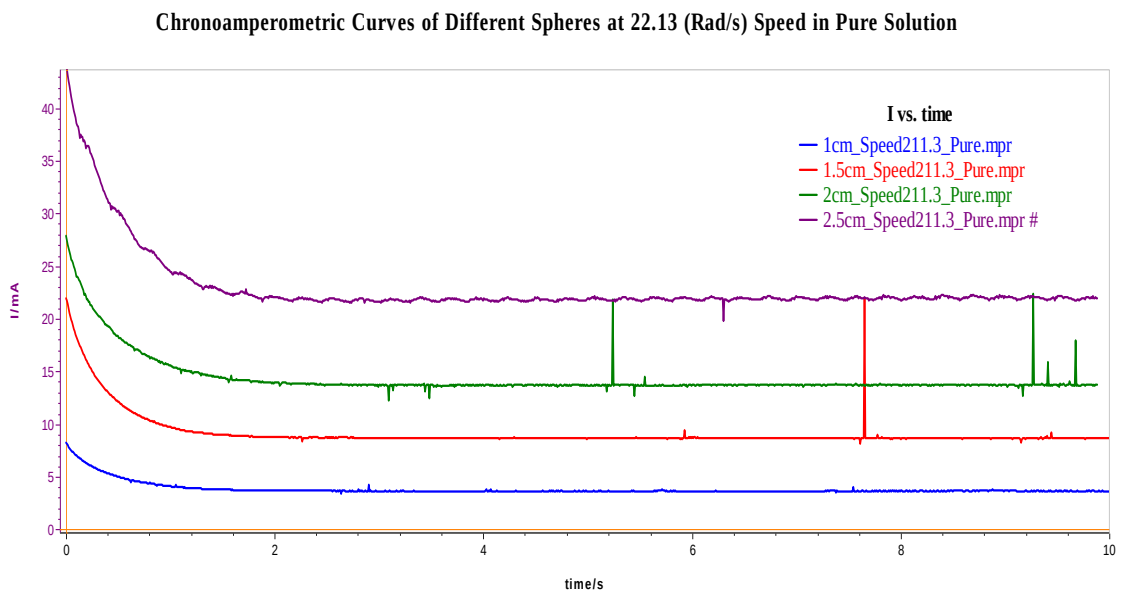

Figure A5: Chronaperometric curves of different spheres at 22.13 (Rad/s) speed in pure solution

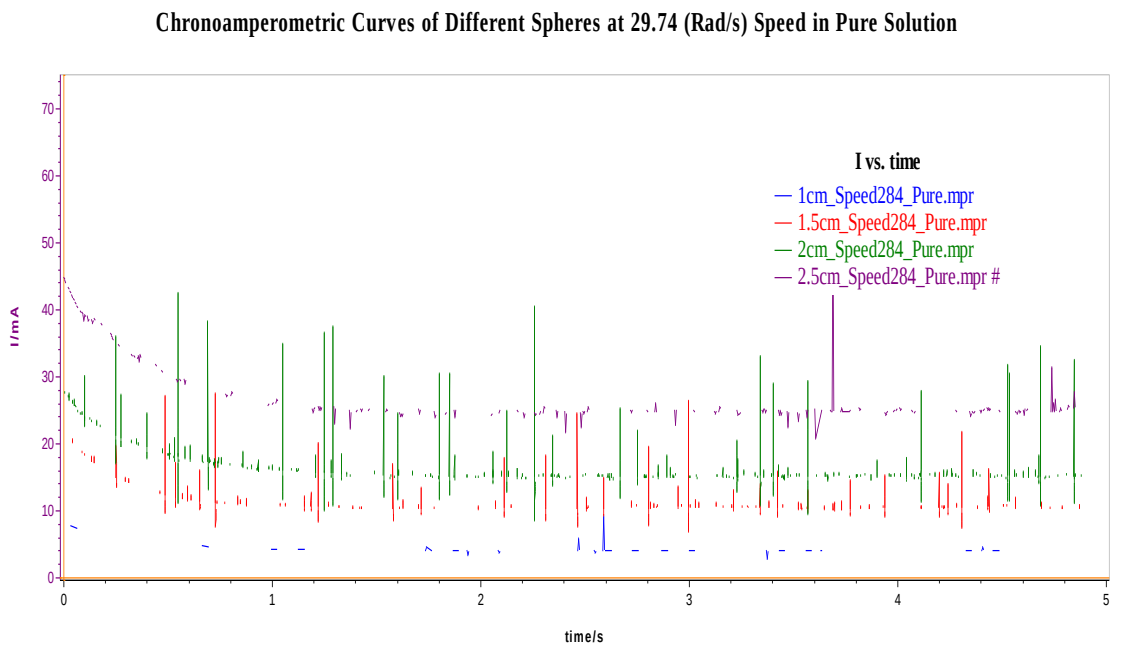

Figure A6: Chronaperometric curves of different spheres at 29.74 (Rad/s) speed in pure solution

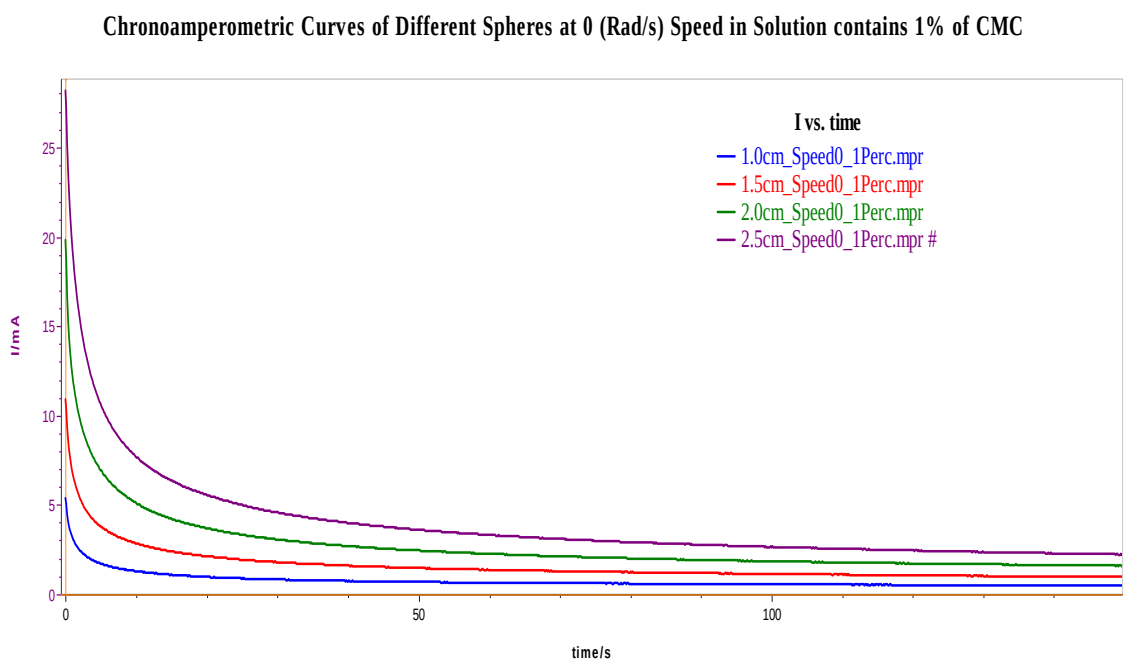

Figure A7: Chronaperometric curves of different spheres at 0 (Rad/s) speed in solution contains 1% of CMC

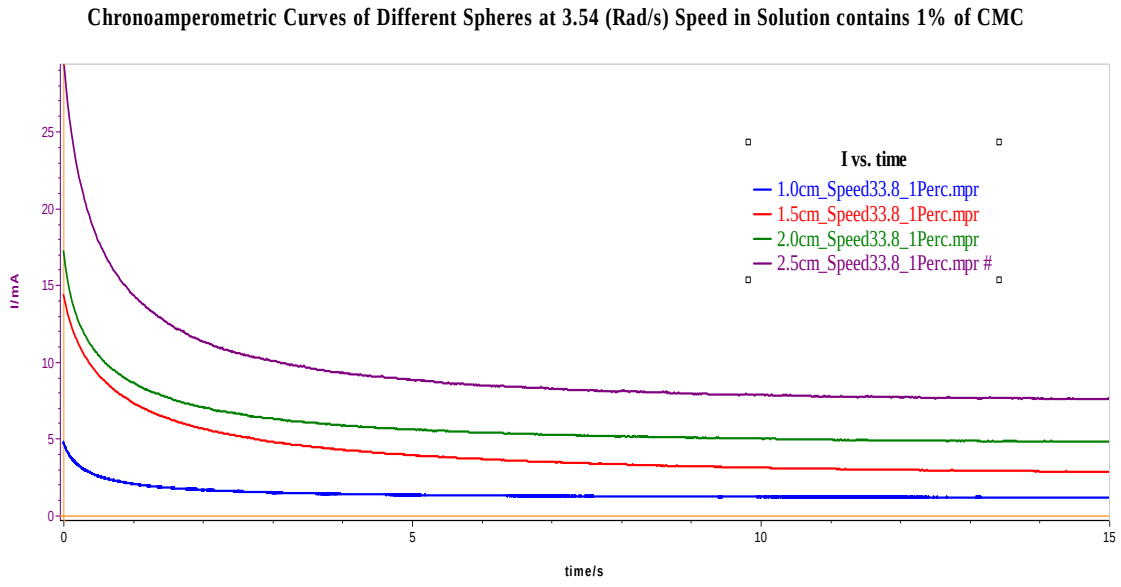

Figure A8: Chronaperometric curves of different spheres at 3.54 (Rad/s) speed in solution contains 1% of CMC

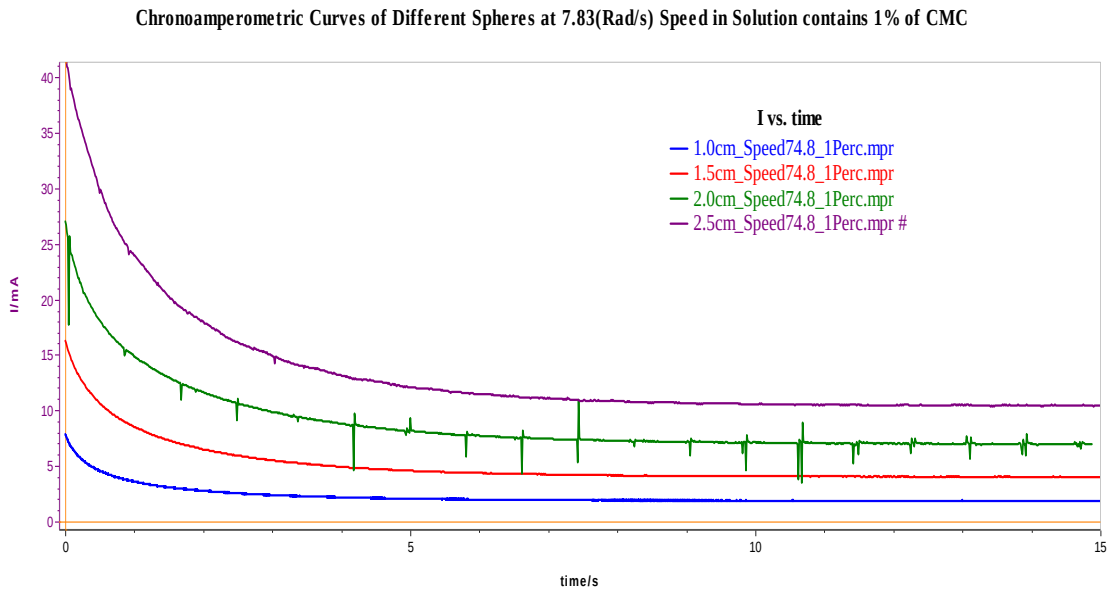

Figure A9: Chronaperometric curves of different spheres at 7.83 (Rad/s) speed in solution contains 1% of CMC

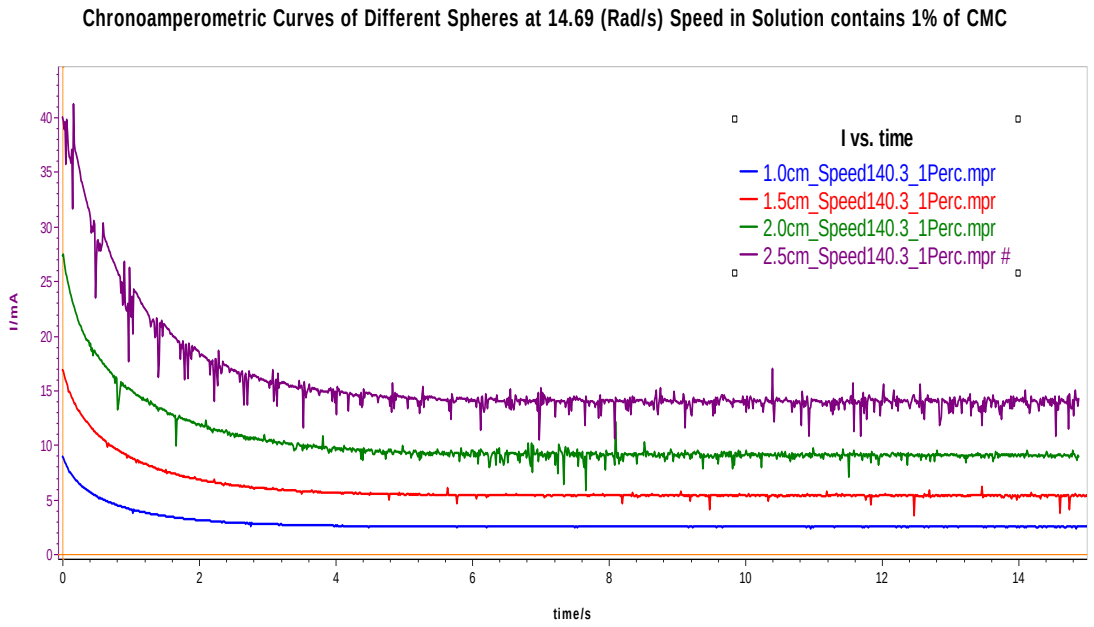

Figure A10: Chronaperometric curves of different spheres at 14.69 (Rad/s) speed in solution contains 1% of CMC

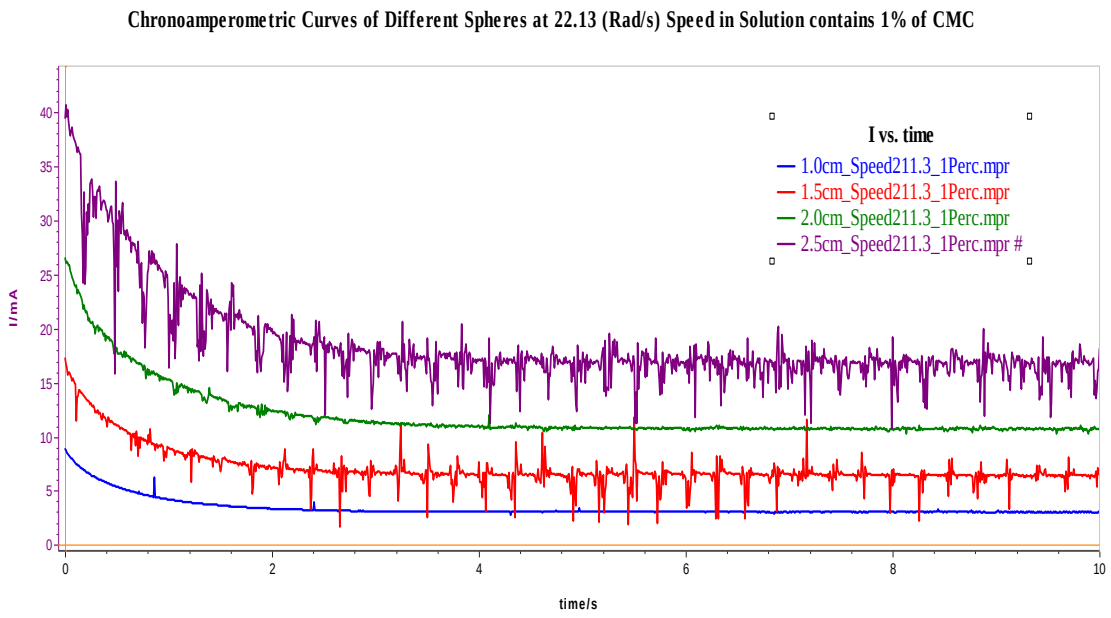

Figure A11: Chronaperometric curves of different spheres at 22.13 (Rad/s) speed in solution contains 1% of CMC

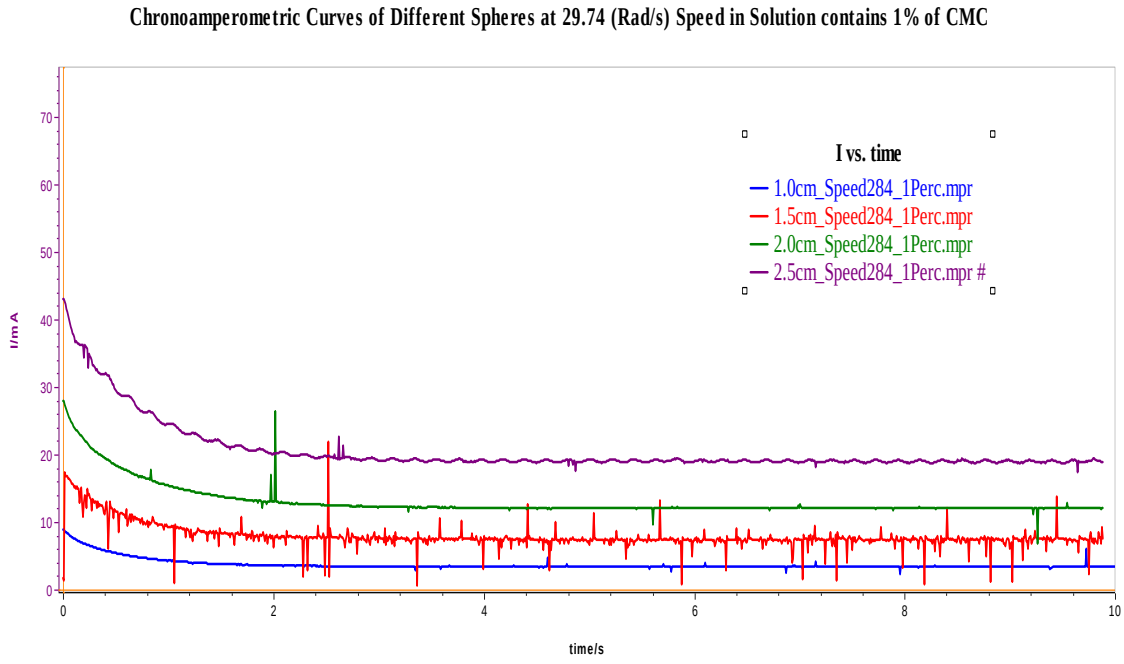

Figure A12: Chronaperometric curves of different spheres at 29.74 (Rad/s) speed in solution contains 1% of CMC

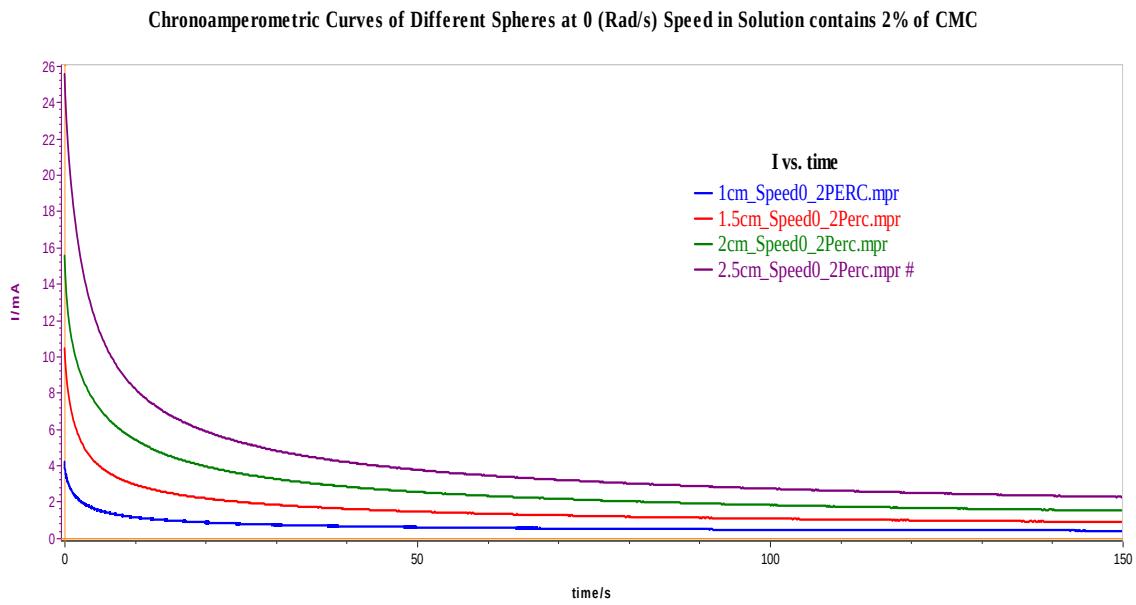

Figure A13: Chronaperometric curves of different spheres at 0 (Rad/s) speed in solution contains 2% of CMC

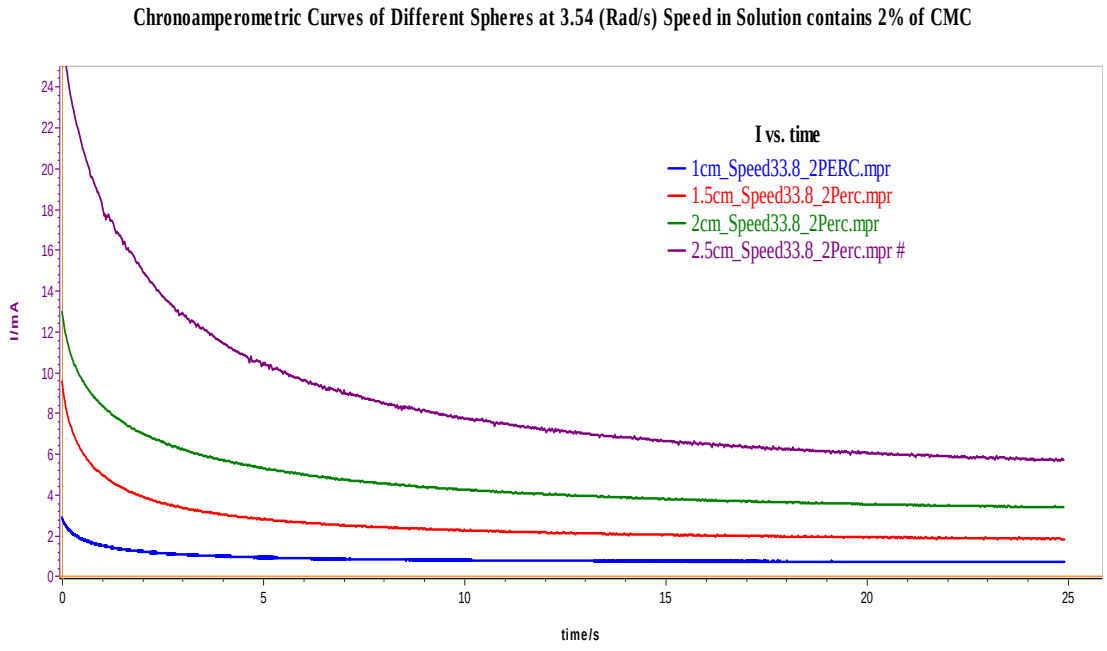

Figure A14: Chronaperometric curves of different spheres at 3.54 (Rad/s) speed in solution contains 2% of CMC

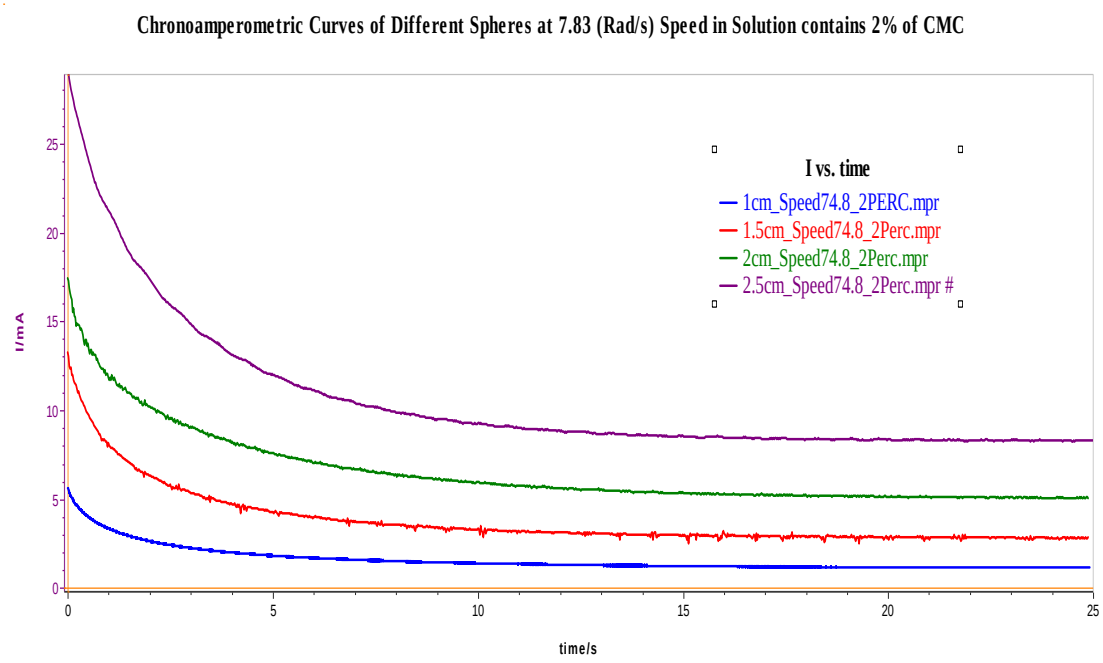

Figure A15: Chronaperometric curves of different spheres at 7.83 (Rad/s) speed in solution contains 2% of CMC

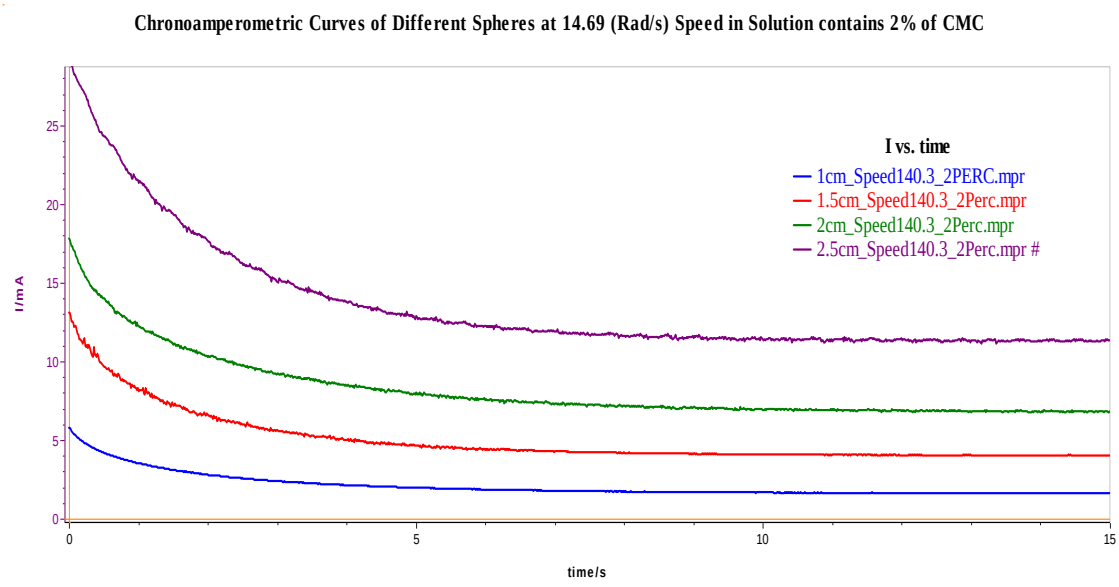

Figure A16: Chronaperometric curves of different spheres at 14.69 (Rad/s) speed in solution contains 2% of CMC

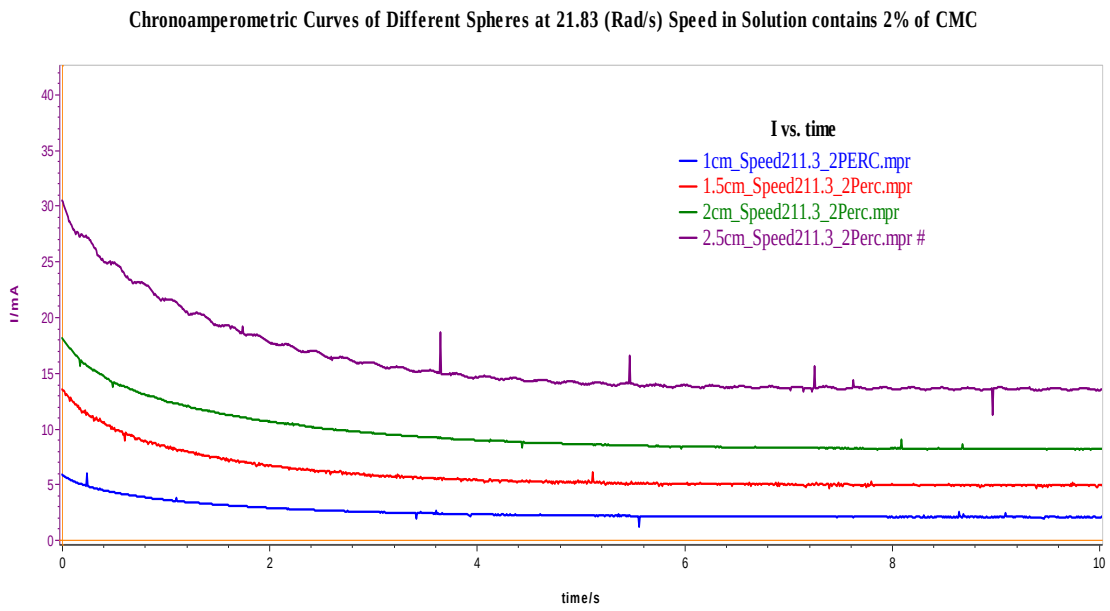

Figure A17: Chronaperometric curves of different spheres at 22.83 (Rad/s) speed in solution contains 2% of CMC

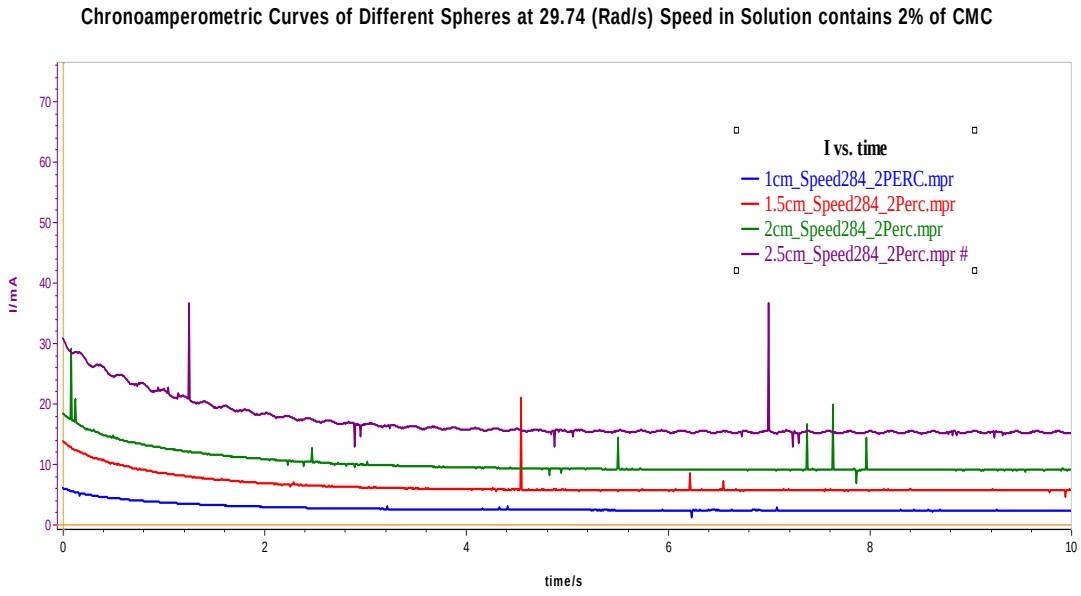

Figure A18: Chronaperometric curves of different spheres at 29.74 (Rad/s) speed in solution contains 2% of CMC

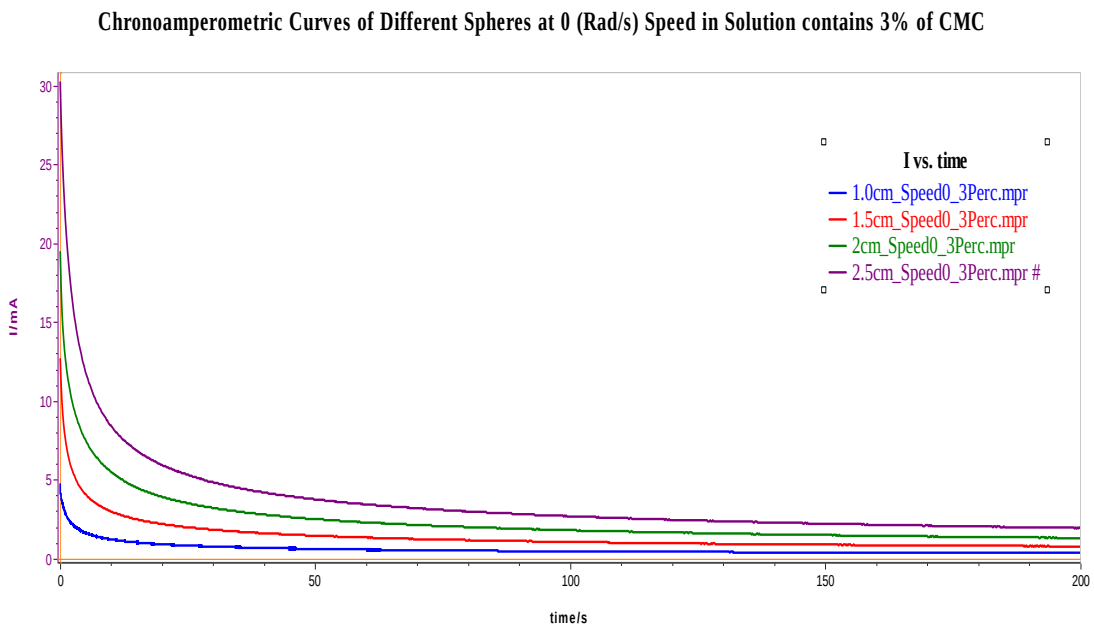

Figure A19: Chronaperometric curves of different spheres at 0.0 (Rad/s) speed in solution contains 3% of CMC

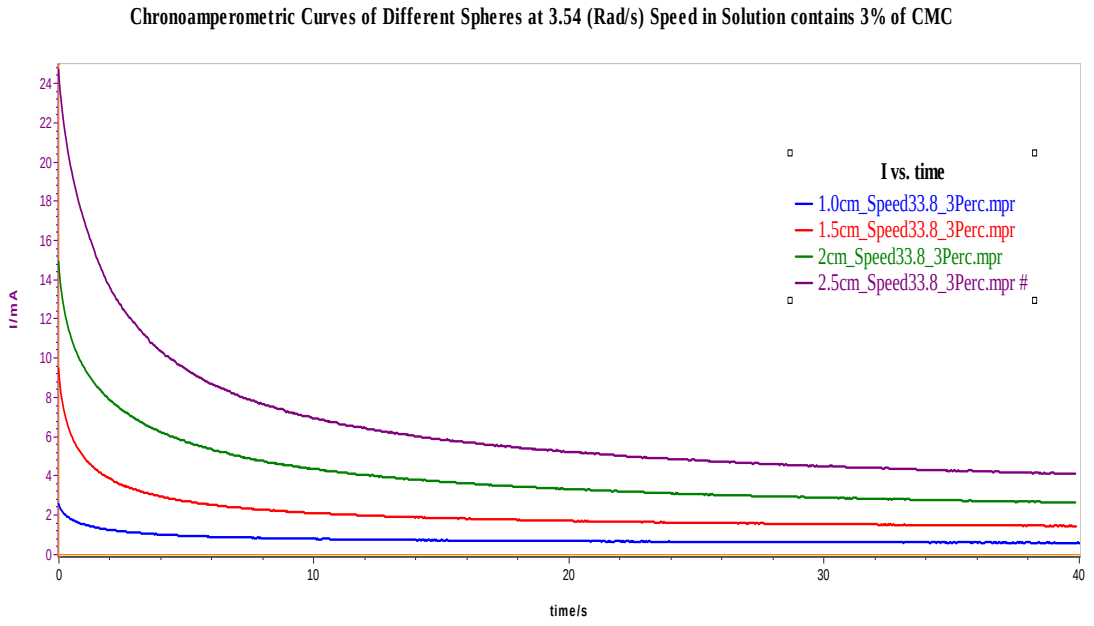

Figure A20: Chronaperometric curves of different spheres at 3.54 (Rad/s) speed in solution contains 3% of CMC

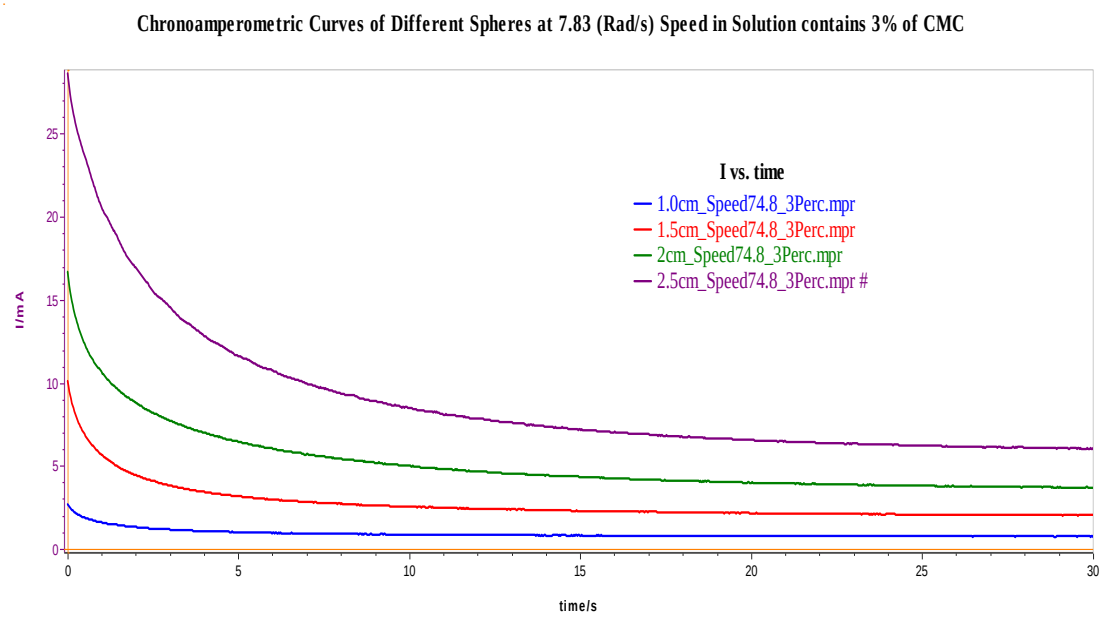

Figure A21: Chronaperometric curves of different spheres at 7.83 (Rad/s) speed in solution contains 3% of CMC

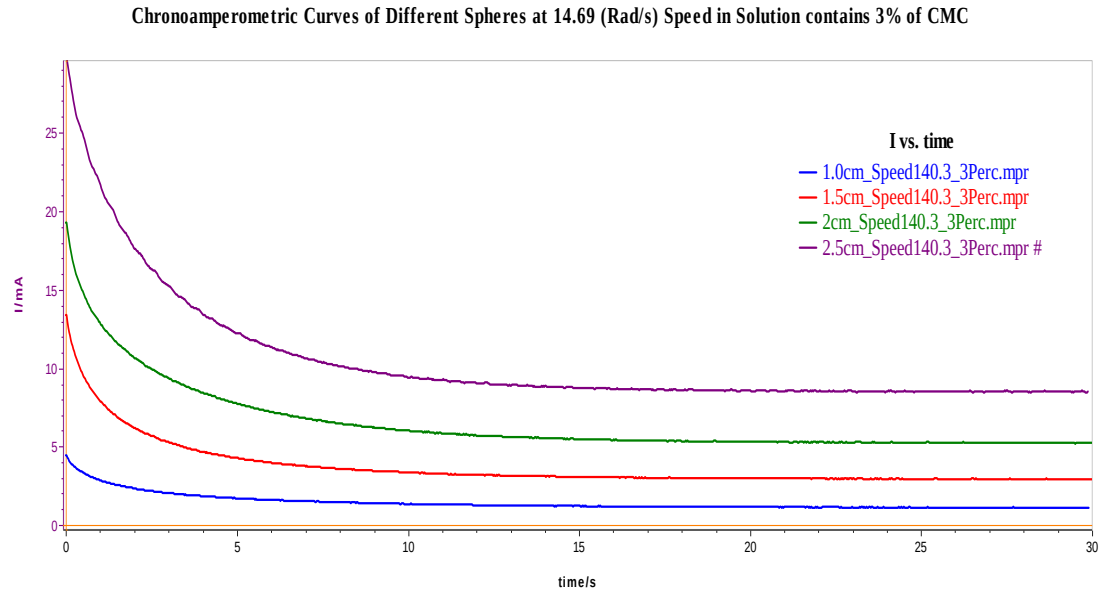

Figure A22: Chronaperometric curves of different spheres at 14.69 (Rad/s) speed in solution contains 3% of CMC

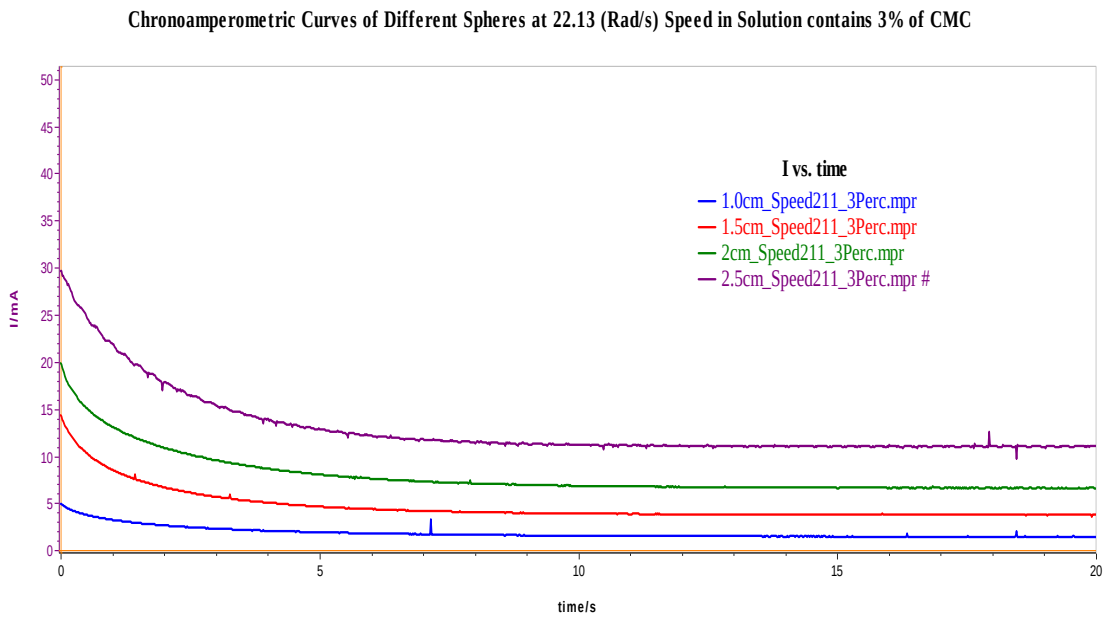

Figure A23: Chronaperometric curves of different spheres at 22.13 (Rad/s) speed in solution contains 3% of CMC

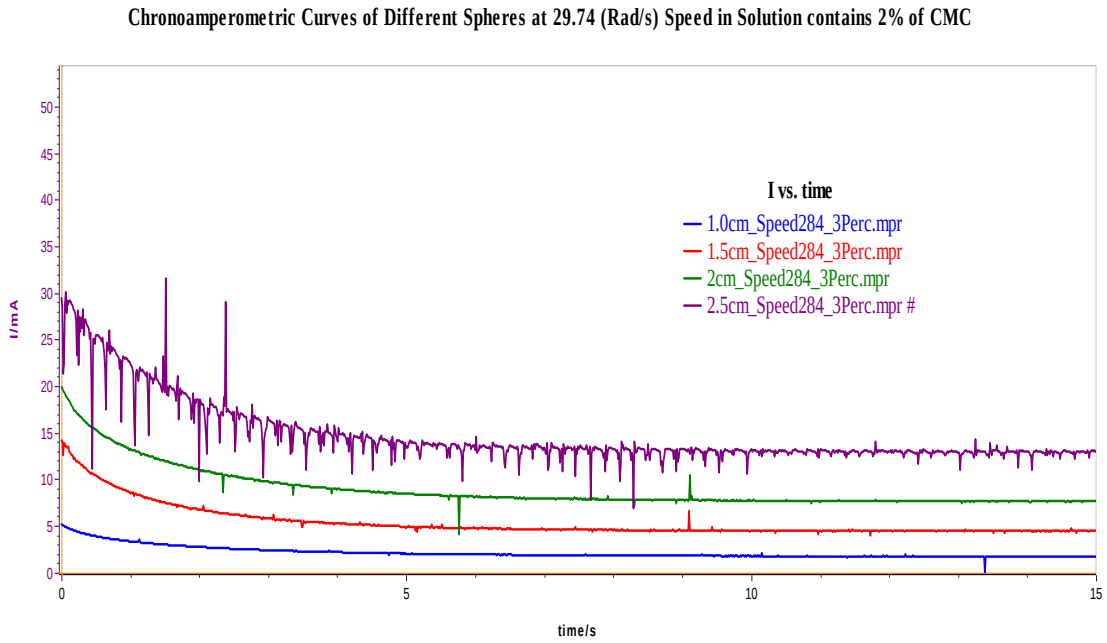

Figure A24: Chronaperometric curves of different spheres at 29.74 (Rad/s) speed in solution contains 3% of CMC

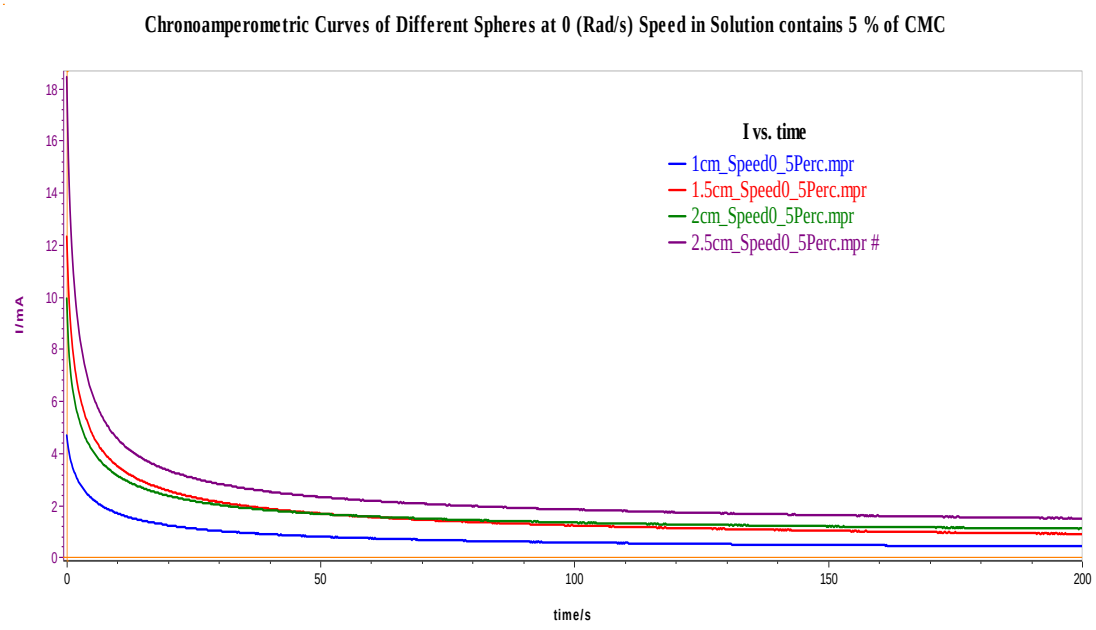

Figure A25: Chronaperometric curves of different spheres at 0.0 (Rad/s) speed in solution contains 5% of CMC

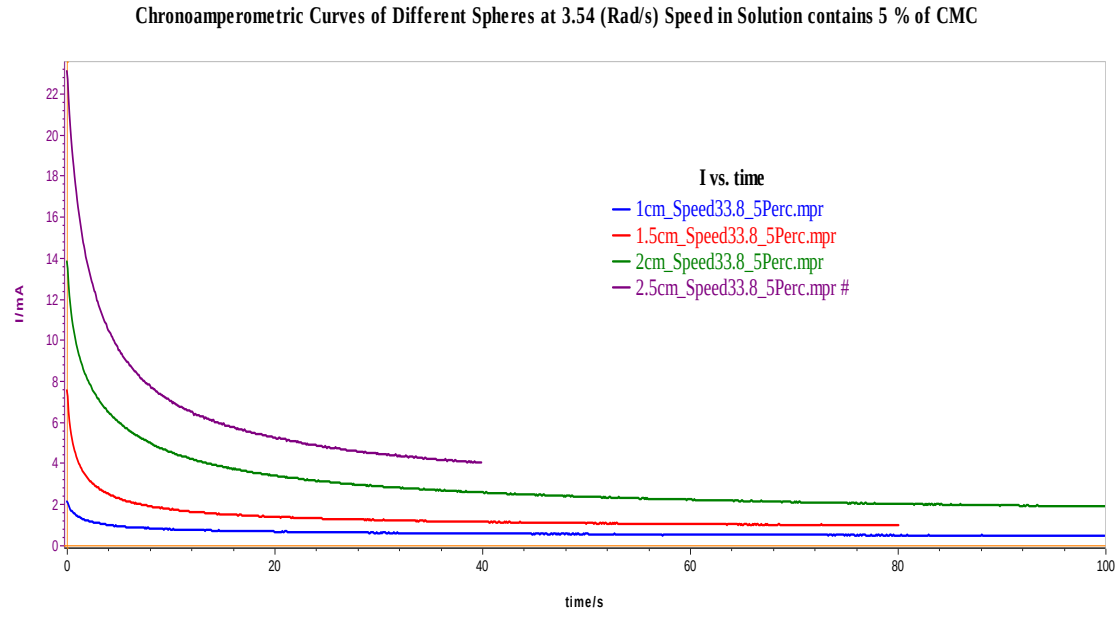

Figure A26: Chronaperometric curves of different spheres at 3.54 (Rad/s) speed in solution contains 5% of CMC

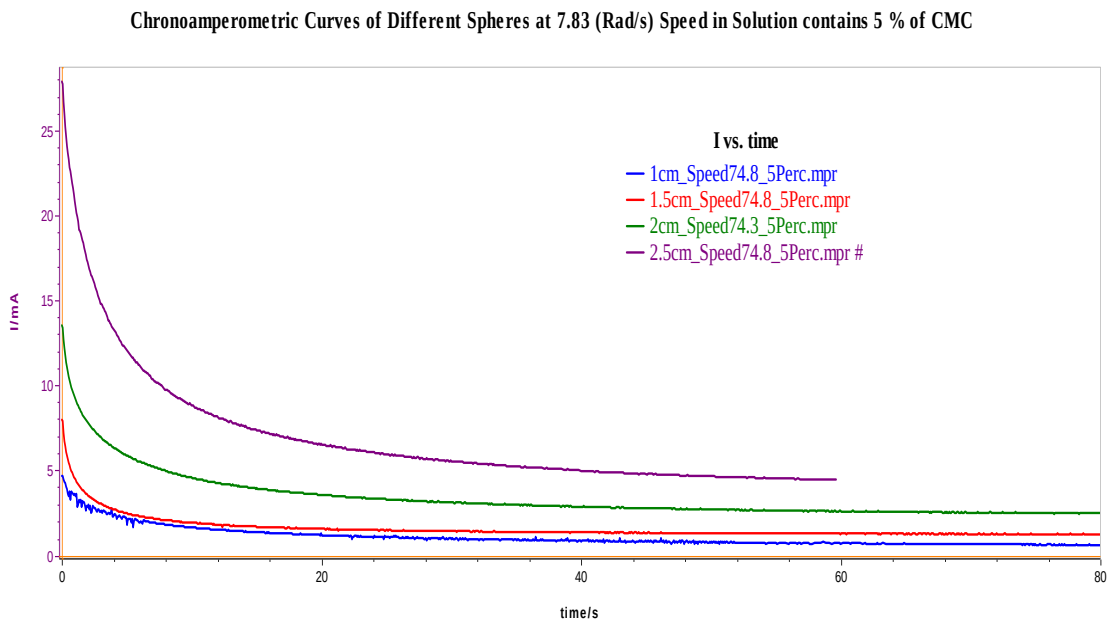

A27: Chronaperometric curves of different spheres at 7.83 (Rad/s) speed in solution contains 5% of CMC

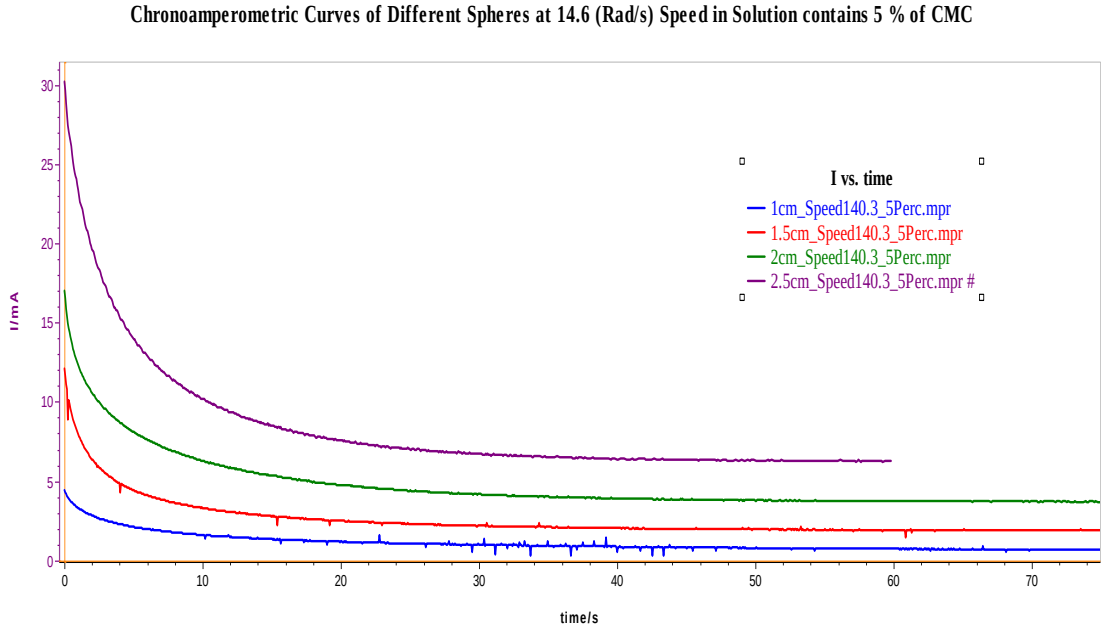

A28: Chronaperometric curves of different spheres at 14.69 (Rad/s) speed in solution contains 5% of CMC

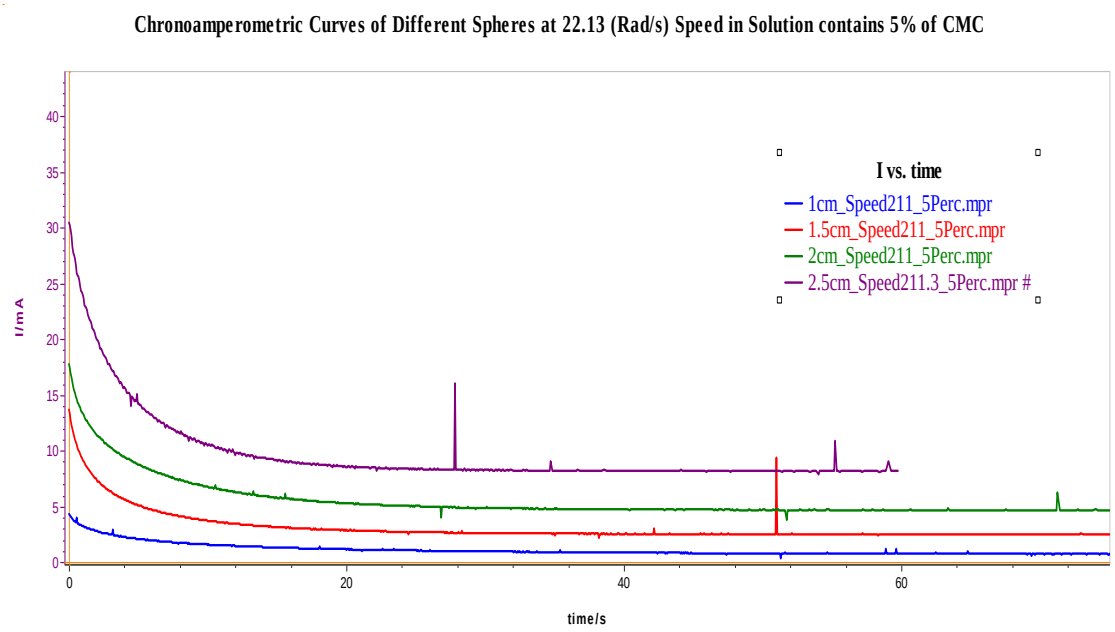

A29: Chronaperometric curves of different spheres at 22.13 (Rad/s) speed in solution contains 5% of CMC

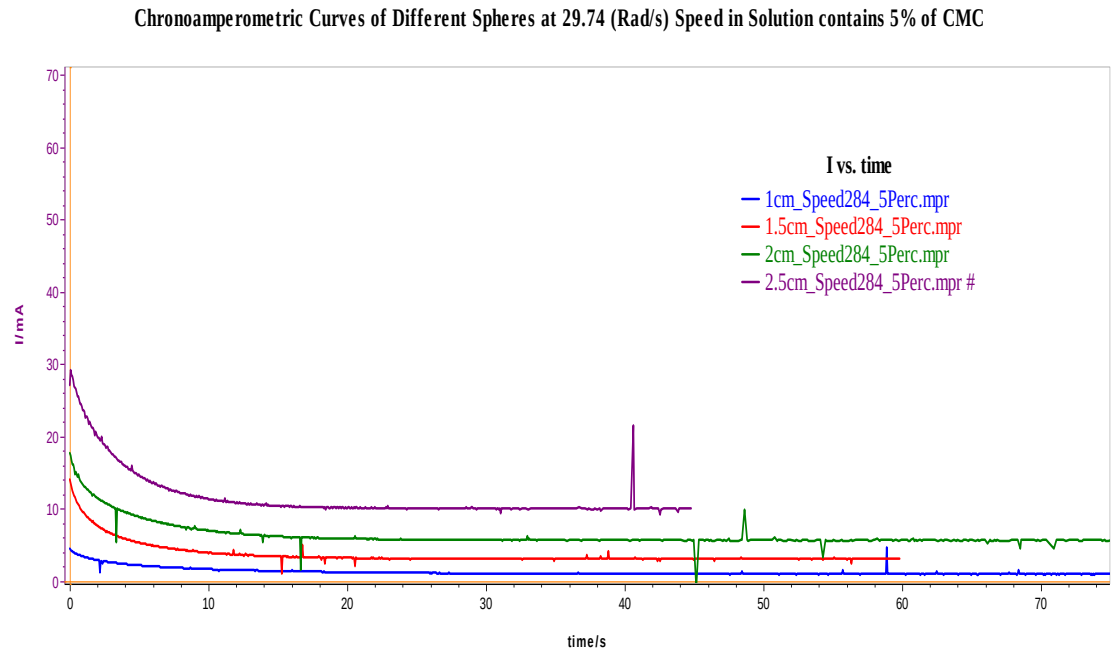

A30: Chronaperometric curves of different spheres at 29.74 (Rad/s) speed in solution contains 5% of CMC

Vitae

Name	:Abdullah Mohsen Mubarak Baduraig
Nationality	:Saudi
Date of Birth	:8/10/1985
Email	:a.baduraig@hotmail.com
Address	: King Fhad University of Petroleum & Minerals Dhahran 31261, Kingdom of Saudi Arabia
Mobile No	: +966506853499

Academic Background : B. S. Chemical Engineering (2008)
King Fhad University of Petroleum & Minerals
Dhahran 31261, Kingdom of Saudi Arabia
M.S. Chemical Engineering (2013)
King Fhad University of Petroleum & Minerals
Dhahran 31261, Kingdom of Saudi Arabia